mucosa is a potential source for autologous stem cell therapy for Parkinson's disease. Stem Cells 26:2183–2192.

Novikova LN, Lobov S, Wiberg M, Novikov LN. 2011. Efficacy of olfactory ensheathing cells to support regeneration after spinal cord injury is influenced by method of culture preparation. Exp Neurol 229: 132–142.

Ohnishi Y, Iwatsuki K, Shinzawa K, Ishihara M, Moriwaki T, Umegaki M, Kishima H, Yoshimine T. 2013. Adult olfactory sphere cells are a source of oligodendrocyte and Schwann cell progenitors. Stem Cell Res 11:1178–1190.

Oishi Y, Baratta J, Robertson RT, Steward O. 2004. Assessment of factors regulating axon growth between the cortex and spinal cord in organotypic co-cultures: effects of age and neurotrophic factors. J Neurotrauma 21:339–356.

Pastrana E, Moreno-Flores MT, Avila J, Wandosell F, Minichiello L, Diaz-Nido J. 2007. BDNF production by olfactory ensheathing cells contributes to axonal regeneration of cultured adult CNS neurons. Neurochem Int 50:491–498.

Richter M, Westendorf K, Roskams AJ. 2008. Culturing olfactory ensheathing cells from the mouse olfactory epithelium. Methods Mol Biol 438:95–102.

Roisen FJ, Klueber KM, Lu CL, Hatcher LM, Dozier A, Shields CB, Maguire S. 2001. Adult human olfactory stem cells. Brain Res 890: 11–22.

Schaefer ML, Bottger B, Silver WL, Finger TE. 2002. Trigeminal collaterals in the nasal epithelium and olfactory bulb: a potential route for direct modulation of olfactory information by trigeminal stimuli. J Comp Neurol 444:221–226.

Tome M, Lindsay SL, Riddell JS, Barnett SC. 2009. Identification of nonepithelial multipotent cells in the embryonic olfactory mucosa. Stem Cells 27:2196–2208.

Vigers AJ, Bottger B, Baquet ZC, Finger TE, Jones KR. 2003. Neurotrophin-3 is expressed in a discrete subset of olfactory receptor neurons in the mouse. J Comp Neurol 463:221–235.

Windus LC, Lineburg KE, Scott SE, Claxton C, Mackay-Sim A, Key B, St. John JA. 2010. Lamellipodia mediate the heterogeneity of central olfactory ensheathing cell interactions. Cell Mol Life Sci 67:1735–1750.

Windus LC, Chehrehasa F, Lineburg KE, Claxton C, Mackay-Sim A, Key B, St. John JA. 2011. Stimulation of olfactory ensheathing cell motility enhances olfactory axon growth. Cell Mol Life Sci 68:3233–3247.

Winstead W, Marshall CT, Lu CL, Klueber KM, Roisen FJ. 2005. Endoscopic biopsy of human olfactory epithelium as a source of progenitor cells. Am J Rhinol 19:83–90.

Woodhall E, West AK, Chuah MI. 2001. Cultured olfactory ensheathing cells express nerve growth factor, brain-derived neurotrophic factor, glia cell line-derived neurotrophic factor and their receptors. Brain Res Mol Brain Res 88:203–213.

Olfactory Mucosal Transplantation After Spinal Cord Injury Improves Voiding Efficiency by Suppressing Detrusor-Sphincter Dyssynergia in Rats

Jiro Nakayama, Tetsuya Takao, Hiroshi Kiuchi, Keisuke Yamamoto, Shinichiro Fukuhara, Yasushi Miyagawa, Masanori Aoki, Koichi Iwatsuki, Toshiki Yoshimine, Masaki Ueno, Toshihide Yamashita, Norio Nonomura, Akira Tsujimura* and Akihiko Okuyama

From the Departments of Urology (JN, TT, HK, KY, SF, YM, KI, NN, AT, AO), Neurosurgery (MA, KI, TY) and Molecular Neuroscience (MU, TY), Osaka University Graduate School of Medicine, Suita, Japan

Purpose: Several recent studies showed that olfactory mucosal transplantation after spinal cord injury promotes extensive regeneration of the injured spinal cord. We examined the efficacy of olfactory mucosal transplantation for bladder dysfunction after spinal cord injury in rats.

Materials and Methods: In adult female rats the Th9-10 spinal cord was completely transected, followed by olfactory mucosal transplantation or gelatin sponge filling as the control. Each group was examined by cystometrogram and external urethral sphincter electromyogram. Calcitonin gene-related peptide and growth associated protein 43 double positive expression in the L6/S1 dorsal horn was evaluated by immunohistochemistry. Transplant sites were examined by immunohistochemistry with antibodies against neurofilament M and neuronal class III β-tubulin.

Results: On cystometrogram voiding efficiency was significantly higher in the transplantation group than in controls. On external urethral sphincter electromyogram with simultaneous cystometrogram the transplantation group showed a larger ratio of interburst silent periods to burst activity duration and a greater number of high frequency oscillations. In the transplantation group calcitonin gene-related peptide and growth associated protein 43 double positive expression in the L6/S1 dorsal horn was less dense than in controls. The transplantation group showed strong neurofilament M and neuronal class III β-tubulin expression at the transplant site.

Conclusions: Olfactory mucosal transplantation after spinal cord injury weakened external urethral sphincter excessive bursting and increased the urethral opening to improve voiding efficiency. Olfactory mucosal transplantation may modify emergence of the spinal micturition reflex after spinal cord injury. Transplantation resulted in new axons growing at the transplant site, implying the possible existence of interneuron bridging across the injured spinal cord.

Key Words: urethra, spinal cord injuries, olfactory mucosa, transplantation, urination disorders

Abbreviations and Acronyms

CGRP = calcitonin gene-related peptide
CMG = cystometrogram
DSD = detrusor-sphincter-dyssynergia
EMG = electromyogram
EUS = external urethral sphincter
GAP43 = growth associated protein 43
GFAP = glial fibrillary acidic protein
HFO = high frequency oscillation
ICI = intercontraction interval
IP = intravesical pressure
NFM = neurofilament M
OEC = olfactory ensheathing cell
OM = olfactory mucosa
OMT = olfactory mucosal transplantation
PBS = phosphate buffered saline
PVR = post-void residual urine volume
SCI = spinal cord injury
SP/P2 = interburst silent periods-to-phase 2 ratio
TUJ-1 = neuronal class III β-tubulin
VCD = voiding contraction duration
VE = voiding efficiency
VV = voided urine volume

Submitted for publication October 9, 2009.
Study received Osaka University animal ethics committee approval.
* Correspondence: Department of Urology, Osaka University Graduate School of Medicine, 2-2 Yamadaoka, Suita, Osaka 565-0871, Japan (telephone: +81-6-6879-3531; FAX: +81-6-6879-3539; e-mail: akitsuji@uro.med.osaka-u.ac.jp).

0022-5347/10/1842-0775/0
THE JOURNAL OF UROLOGY®

Vol. 184, 775-782, August 2010
Printed in U.S.A.
DOI:10.1016/j.juro.2010.03.105

SPINAL cord injury causes various types of voiding dysfunction depending on injury level or severity.[1] Urinary incontinence, difficult urination, urinary retention requiring catheterization and subsequent urinary infection spoil the quality of life of patients with SCI.

Unlike the peripheral nerves, after the central nerves are injured they can scarcely be repaired since they have poor regenerative ability (intrinsic factor[2,3]) and glial scars such as reactive astrocytes inhibit axonal growth (extrinsic factor[4,5]). To treat voiding dysfunction after SCI only symptomatic therapy is done. To our knowledge no radical treatment is currently available.

To date several cell transplantation therapies for SCI have been studied, including macrophages,[6] Schwann cells,[7] stromal cells derived from bone marrow[8] or adipose tissue[9] and embryonic stem cells.[10] Each has shown efficacy but is not clinically available due to ethical problems or difficulty in extracting tissue.

Recently the olfactory nerve system has been studied as a candidate for SCI treatment. In the mammalian olfactory system neurogenesis continues throughout life. This unique ability is due to OM components, including OECs and neural stem cells. OECs secrete several neurotrophins,[11] inhibit glial scar formation[12,13] and promote axonal regeneration.[14] Neural stem cells in OM differentiate into neurons and OECs.[15–17] Animal studies showed that OMT after SCI promotes extensive regeneration of the injured spinal cord and improves motor function (hind limb movement).[18] OM has advantages for clinical use, in that it is easily extracted by endoscopic surgery, and free of ethical problems and rejection because it is an autograft. A pilot clinical study of OM autografts for human SCI has already started in Portugal.[19] All 7 patients had neurological improvement of sensory and motor function, of whom 2 recovered bladder sensation. However, the mechanisms behind OMT induced improvement in voiding function after SCI have not been precisely studied.

We examined the effect of OMT on neurogenic bladder dysfunction after SCI in rats by CMG and EMG. C-fiber afferents sprouting in the L6/S1 dorsal horn were examined by immunohistochemistry to evaluate emergence of the voiding reflex after SCI. Together with the immunohistochemical appearance of the transplant site we investigated how OMT affects the voiding reflex after SCI.

MATERIALS AND METHODS

All study experimental protocols and procedures met the guidelines of the Japanese Association for Laboratory Animal Science and were approved by the Osaka University animal ethics committee.

Surgical Procedures

SCI and OMT were done as previously described.[18] Adult female Sprague-Dawley®™ rats weighing 200 to 250 gm were anesthetized intraperitoneally using sodium pentobarbital (Dainippon-Sumitomo, Osaka, Japan) (50 mg/kg). After laminectomy at Th8-10 a 2 mm region of the spinal cord at Th9-10 was excised. OM donated from another adult female Sprague-Dawley rat was cut into 0.5 mm section and inserted into the injured spinal cavity (OMT group). SCI controls received Spongel® gelatin sponge filling in the injured spinal cavity. Rats were housed individually after SCI with a 12-hour light/dark cycle, and free access to water and food. They were treated subcutaneously with the antibiotic isepamicin sulfate (Asahi Kasei Pharma, Tokyo, Japan) (20 mg/kg) for 5 days after SCI. Bladders were expressed 2 to 3 times daily until sacrifice.

Cystometrogram

Four days, and 2 and 4 weeks after SCI we examined 5 OMT rats and 5 SCI controls by awake CMG. Cystostomy was done as previously described[20] with modifications. Briefly, after the rats were temporarily anesthetized with isoflurane (Abbott Laboratories, Tokyo, Japan) (2.5% in O_2) a PE-50 polyethylene catheter (BD®) was inserted into the bladder to infuse physiological saline and record IP. The rat was then restrained in a KN-326 Type 3 Ballman cage (Natsume, Seisakusho, Japan). CMG was started 2 hours after surgery to allow the rat to recover from isoflurane anesthesia. Before measuring values saline was infused into the bladder for 2 hours at a constant rate of 0.08 ml per minute. The signal from the pressure transducer was amplified by an MEG-6108 multichannel amplifier (Nihon Koden, Tokyo, Japan), sampled at 100Hz and acquired on the computer using PowerLab® Chart 5. Voided urine was collected in a vessel under the cage. Volume was measured at each voiding and average volume was calculated as VV. After 5 voiding contractions the infusion pump was turned off and residual saline was withdrawn to measure PVR. We evaluated maximum IP, ICI, VV and PVR as well as VE using the equation, VE = VV/VV + PVR.

EUS Electromyogram

We examined 4 OMT rats and 4 SCI controls by EUS-EMG during CMG 4 weeks after the procedure. EMG with simultaneous CMG was done in a new cohort under the same conditions as described for CMG with the awake rat restrained in a Ballman cage. A pair of finely twisted stainless electrodes (Unique Medical, Tokyo, Japan) 0.25 mm in diameter were placed bilaterally via a percutaneous approach beside the urethra. EMG activity was amplified 2,000-fold with an AB-611J/JB-611J EMG amplifier (Nihon Koden) and filtered (high and low frequency cutoffs at 10,000 and 50 Hz, respectively). EUS-EMGs with simultaneous CMGs were sampled at 10,000 Hz using PowerLab Chart 5.

As previously described,[21] for analysis we divided EUS-EMGs with CMGs into 4 phases (fig. 1). Briefly, phase 1 is a storage phase in which IP increases, followed by phase 2, in which voiding contraction starts and IP gradually de-

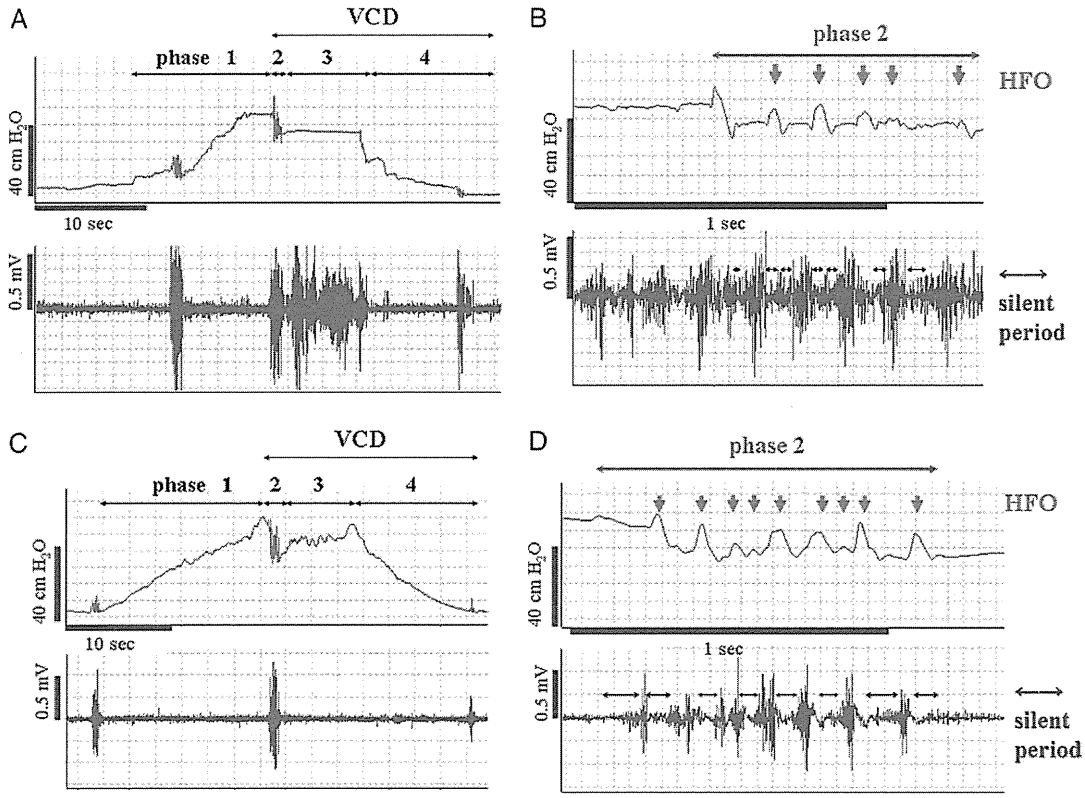

Figure 1. Representative EUS-EMGs with spontaneous CMG in SCI controls (*A* and *B*) and OMT rats (*C* and *D*) 4 weeks after SCI show CMG phases 1 to 4 (*A* and *C*) and phase 2 analysis (*B* and *D*). In OMT rats HFO count was greater and EMG showed milder bursting than in controls.

creases with HFO. EUS-EMG shows phasic activity during phase 2. HFOs are interpreted as IP fluctuations generated by phasic bursting activity of the external urethral sphincter, which is needed to facilitate urine voiding in rats.[22] In phase 3 IP increased again and then decreased to baseline in phase 4. We evaluated SP/P2, the number of HFOs in phase 2 and the duration from the beginning of phase 2 to the end of phase 4 (VCD). CMG parameters were also evaluated in this EMG cohort. At 4 weeks 9 SCI controls and 9 OMT rats were available for CMG evaluation.

Tissue Preparation

Four weeks after SCI 4 OMT rats and 4 SCI controls were anesthetized with sodium pentobarbital (100 mg/kg intraperitoneally) and sacrificed by intracardiac perfusion with 200 ml physiological saline, followed by 200 ml 4% paraformaldehyde fixative in 0.2M PBS. The spinal cord was removed and post fixed for 12 hours in the same fixative at 4C, followed by cryoprotection in phosphate buffered 30% sucrose solution for 12 hours. The spinal cord was blocked, embedded in Tissue-TEK® O.C.T.™ compound and kept at −80C before being cut into sections. In 4 normal intact rats the spinal cord was removed and prepared in the same procedure for comparison.

L6/S1 Spinal Cord Dorsal Horn

To evaluate emergence of the voiding reflex after SCI peptidergic C-fiber afferents sprouting in the L6/S1 dorsal horn were examined by immunohistochemistry using an antibody against CGRP and an antibody against GAP43.

The L6/S1 spinal cord of rats in the 2 SCI groups and normal rats was cut into 20 μm coronal sections in a cryostat and mounted on Matsunami adhesive silane coated glass slides (Matsunami Glass, Kishiwada City, Japan). After blocking with 10% bovine serum albumin (Sigma-Aldrich®) with 0.3% Triton-X (Nacalai Tesque, Kyoto, Japan) for 1 hour at room temperature the sections were incubated overnight at 4C with guinea pig polyclonal antibody against CGRP (T-5053, Peninsula Laboratories, San Carlos, California) (1:1,000) and mouse monoclonal antibody against GAP43 (MAB347, Millipore®) (1:2,000) for double immunostaining. After rinsing in PBS with 0.05% Tween-20 sections were incubated for 1 hour at room temperature with the secondary antibody, Alexa Fluor® 488 goat anti-guinea pig IgG for CGRP and Alexa Fluor 568 goat anti-mouse IgG (Molecular Probes®) (each 1:500) for GAP43.

Transplant Site

The existence of new axons at the transplant site in the 2 SCI groups was evaluated by immunohistochemistry using rabbit polyclonal antibodies against TUJ-1 (PRB-435P, Covance ®) (1:500) and rabbit polyclonal antibodies against NFM (AB1987, Millipore) (1:200). Immunohistochemistry using mouse monoclonal antibodies against

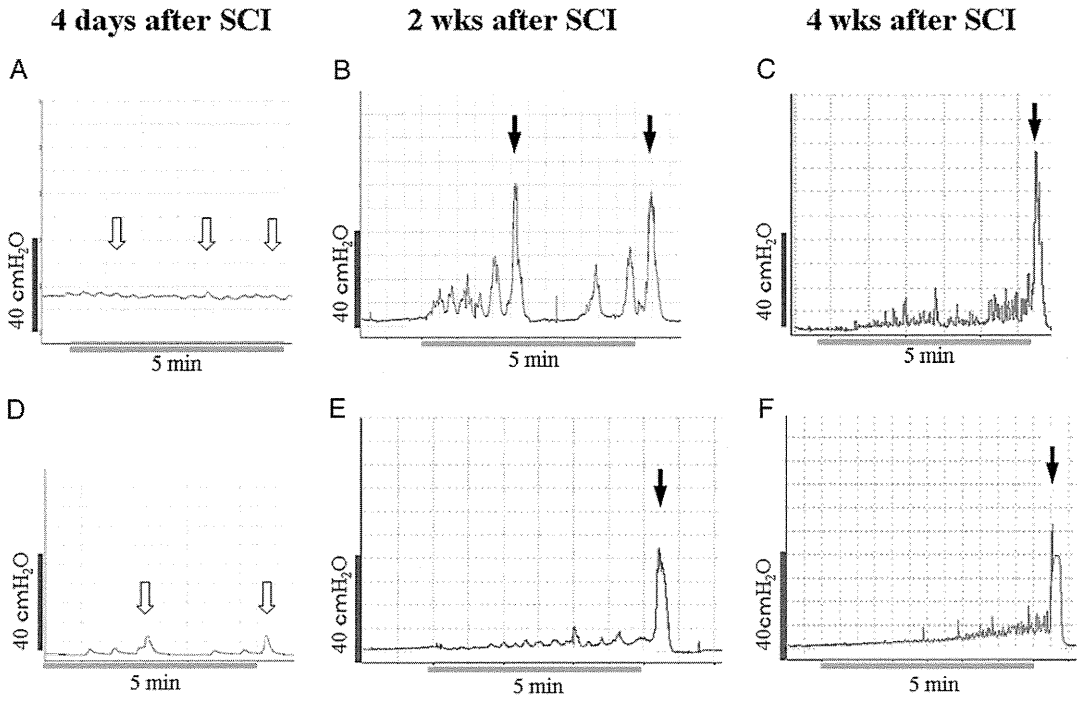

Figure 2. Representative CMG charts in SCI controls (*A* to *C*) and OMT rats (*D* to *F*). Neither group showed obvious voiding contractions (black arrows) 4 days after SCI (*A* and *D*). Urine was expressed by overflowing at certain intervals (open arrows). Voiding contractions emerged in controls 2 weeks after SCI with preceding nonvoiding contractions (*B*). Controls had longer ICI at 4 (*C*) than at 2 (*B*) weeks after SCI. In OMT rats ICI tended to be longer and maximum voiding pressure tended to be less than in controls 2 and 4 weeks after SCI but this was not significant (*E* and *F*).

GFAP (G-3893, Sigma®) (1:200) was also done to evaluate glial scar formation.

Th7-10 spinal cord was cut longitudinally into 20 μm sections in a cryostat and mounted onto Matsunami adhesive silane coated glass slides. After the same blocking procedures as described, sections were incubated overnight at 4C with primary antibodies. For double immunostaining a combination of antibodies against TUJ-1 and GFAP, and antibodies against NFM and GFAP served as primary antibodies. After rinsing with PBS-Tween the sections were incubated for 1 hour at room temperature with secondary antibodies, including Alexa Fluor 568 goat anti-rabbit IgG (1:500) for TUJ-1 and NFM, and Alexa Fluor 488 goat anti-mouse IgG (1:500) for GFAP.

Image Analysis

Images were captured using an all in 1 BZ-8000 fluorescence microscope (Keyence, Osaka, Japan) with a 20× objective. Images were analyzed using BZ Analyzer Software (Keyence), Image J (http://rsb.info.nih.gov/ij) and Photoshop® 7.0. The density of CGRP and GAP43 double positive primary afferent axons in the dorsal horn of the L6/S1 spinal cord (laminae I to IV) was analyzed in 4 SCI rats and 4 normal, spinal intact rats. The image was converted using Image J into pixels on the computer monitor according to a gray scale intensity range of 0—white to 255—black. According to previously described procedures[23,24] the background level was determined in an area of ventral funiculus that did not show immunoreactivity and was used to set the threshold between labeled and background pixels. We randomly chose 5 sections per rat and measured the immunoreactive area to calculate the average as representative data on each.

Statistical Analysis

Urodynamic data were analyzed using Mann-Whitney's U test. Immunohistochemical density data were analyzed using the Kruskal-Wallis test between groups, followed by post hoc analysis with Scheffe's F test. Data are shown as the group mean ± SD with significance considered at 0.05 for all comparisons.

RESULTS

Cystometrogram

Four days after SCI jagged waveforms without obvious voiding contractions were seen on CMG in SCI

Table 1

Parameters	Mean ± SD SCI Control	Mean ± SD OMT
No. HFOs	7.58 ± 2.35	10.67 ± 1.50*
Phase 2 (secs)	1.25 ± 0.42	1.26 ± 0.40
Silent period (secs)	0.67 ± 0.31	0.86 ± 0.36
% SP/P2	52.7 ± 9.00	67.3 ± 8.27*
VCD (secs)	23.38 ± 5.47	19.39 ± 3.64*

* Significantly different (Mann-Whitney U test) $p < 0.05$.

Table 2

Time After SCI Parameters	Mean ± SD SCI Control	Mean ± SD OMT
4 Days:		
ICI (mins)	1.88 ± 0.72	1.99 ± 0.89
Max IP (cm H_2O)	14.02 ± 4.52	18.69 ± 5.41
VV (ml)	0.15 ± 0.06	0.16 ± 0.07
PVR (ml)	3.05 ± 0.45	2.13 ± 0.95
% VE	4.60 ± 1.11	7.44 ± 3.80
2 Wks:		
ICI (mins)	3.35 ± 1.92	5.64 ± 2.46
Max IP (cm H_2O)	43.22 ± 11.17	48.72 ± 17.26
VV (ml)	0.26 ± 0.15	0.45 ± 0.20
PVR (ml)	0.39 ± 0.13	0.16 ± 0.12
% VE	39.6 ± 17.8	75.5 ± 14.9*
4 Wks:		
ICI (mins)	7.15 ± 1.86	8.25 ± 1.92
Max IP (cm H_2O)	59.0 ± 14.3	50.5 ± 6.55
VV (ml)	0.57 ± 0.15	0.66 ± 0.15
PVR (ml)	0.66 ± 0.20	0.28 ± 0.14*
% VE	51.1 ± 15.1	71.7 ± 13.2*

* Significantly different (Mann-Whitney U test $p < 0.05$).

controls and OMT rats (fig. 2, *A* and *D*). Each SCI group urinated by overflowing and only had less than 10% VE (table 1). Two and 4 weeks after SCI each SCI group showed obvious voiding contractions (fig. 2, *B*, *C*, *E* and *F*). There were no significant differences between the groups for ICI or VV but PVR was significantly lower in the OMT group 4 weeks after SCI (mean 0.28 ± 0.14 vs 0.66 ± 0.20 ml) and VE was significantly higher in the OMT group than in controls (mean 71.7% ± 13.2% vs 51.1% ± 15.1%) (table 1).

EUS-EMG and CMG

In the OMT group there were significantly more HFO counts and SP/P2 was significantly higher than in SCI controls. OMT rats had a shorter VCD than SCI controls (table 2 and fig. 1). On EMG in SCI controls EUS excessive bursting appeared in phase 3 (fig. 1, *A*), implying DSD.

L6/S1 Dorsal Horn C-Fiber Afferents

CGRP/GAP43 double positive expression in the L6/S1 dorsal horn, reflecting the sprouting of CGRP positive C fiber afferents, was denser in SCI controls than in normal, spinal intact controls. In OMT rats CGRP/GAP43 double positive expression in the L6/S1 dorsal horn was also denser than in normal controls but less dense than in SCI controls (figs. 3 and 4).

Transplant Site

In OMT rats strong NFM and TUJ-1 expression was observed at the transplant site. GFAP expression accumulated in the caudal and cranial stumps of the injured spinal cord but was scarcely seen at the transplant site (fig. 5, *B* and *D*). In SCI controls the injured site showed neither NFM nor TUJ-1 expression. Sparse GFAP expression was noted in SCI controls, implying the existence of glial scar tissue, such as reactive astrocytes (fig. 5, *A* and *C*).

DISCUSSION

In humans and animals the bladder becomes areflexic immediately after complete SCI above the

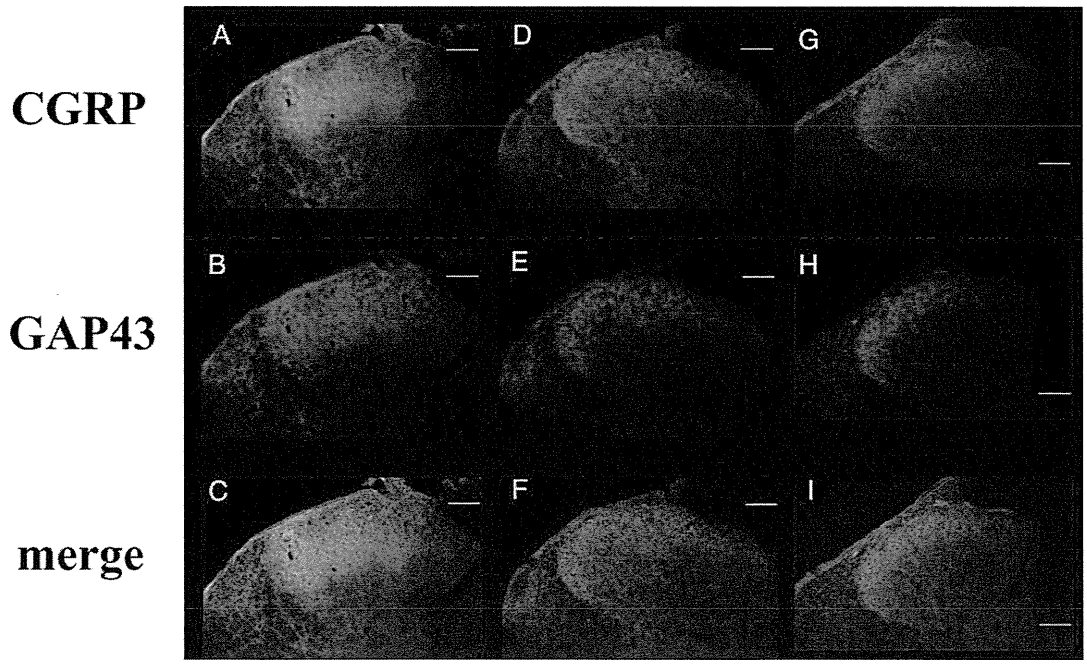

Figure 3. CGRP (green areas) and GAP43 (red areas) positive afferent terminal in L6/S1 dorsal horn in SCI controls (*A* to *C*), OMT rats (*D* to *F*) and normal controls (*G* to *I*). Double positive expression was noted (yellow areas) in merged images (*merge*). Scale bars represent 100 μm.

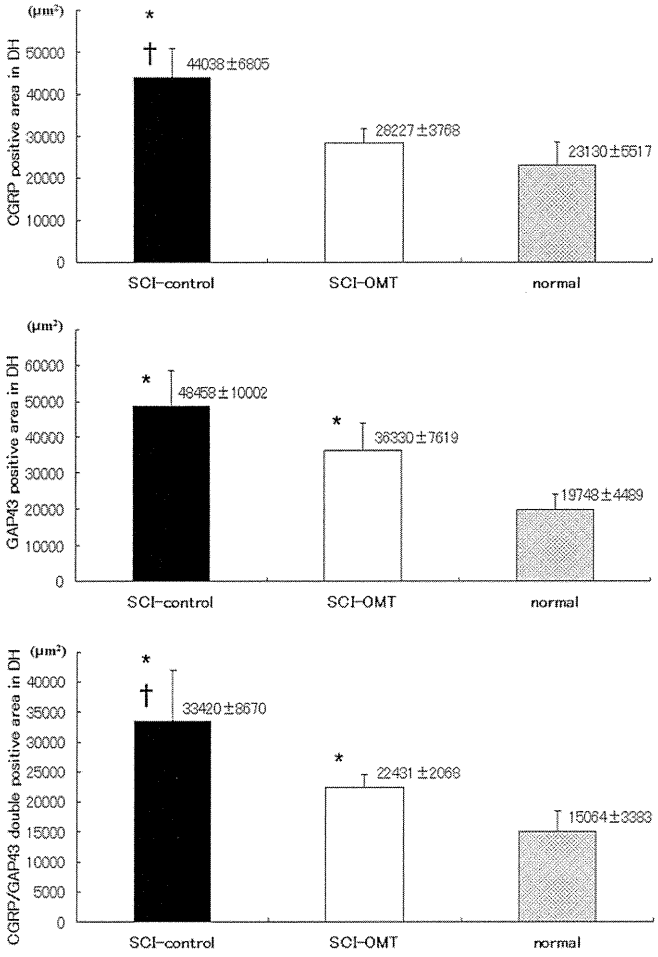

Figure 4. Density of CGRP, GAP43 and CGRP/GAP43 double positive primary afferent axons in dorsal horn (*DH*) laminae I to IV of L6/S1 spinal cord. Values indicate mean ± SD calculated area. Double positive expression in OMT rats was denser than in normal controls but significantly less dense than in SCI controls. Asterisk indicates $p < 0.05$ vs normal controls. Dagger indicates $p < 0.05$ vs OMT.

lumbosacral spinal region and several weeks after SCI the spinal micturition reflex emerges.[23] This compensatory voiding generally results in inefficient bladder emptying since detrusor contractions are involuntary and lacking in coordination with a hypertonic sphincter. This is known as DSD. The morphological change in the bladder due to difficult urination after SCI also worsens voiding function.[25]

In our study voiding function in OMT rats and SCI controls showed time dependent recovery, as mentioned. However, OMT rats had better VE on CMG than SCI controls 2 and 4 weeks after SCI. External urinary sphincter EMG and simultaneous CMG in OMT rats 4 weeks after SCI showed more HFO counts, more silent periods and shorter VCD. In previous studies HFOs were evaluated on CMG only in anesthetized rats. Cruz and Downie noted single bladder pressure with no HFOs on previous CMG in awake female rats but the lack of HFO detection on CMG in awake rats was a technical problem and in awake condition the effect of EUS on bladder pressure may be masked by tonic detrusor pressure or an abdominal muscle contribution.[26] HFOs emerged on CMG in awake SCI rats in our study. SCI rats may lack perception and voluntary movements in the lower body, which is associated with SCI dermatome distribution, and so the artifact on awake CMG may be less than normal. Thus, HFOs may be an index of urethral opening or fluid evacuation in the micturition phase in SCI rats. Briefly, our results imply that SCI with OMT weakened the excessive EUS burst duration and increased urethral opening during voiding, thus improving VE.

The voiding reflex after SCI is considered to partially depend on the plasticity of C-fiber bladder afferent pathways.[23] Afferent pathways induce the efferent response by reorganizing spinal interneurons connected to sacral parasympathetic motoneurons for bladder contraction[27] and interneurons

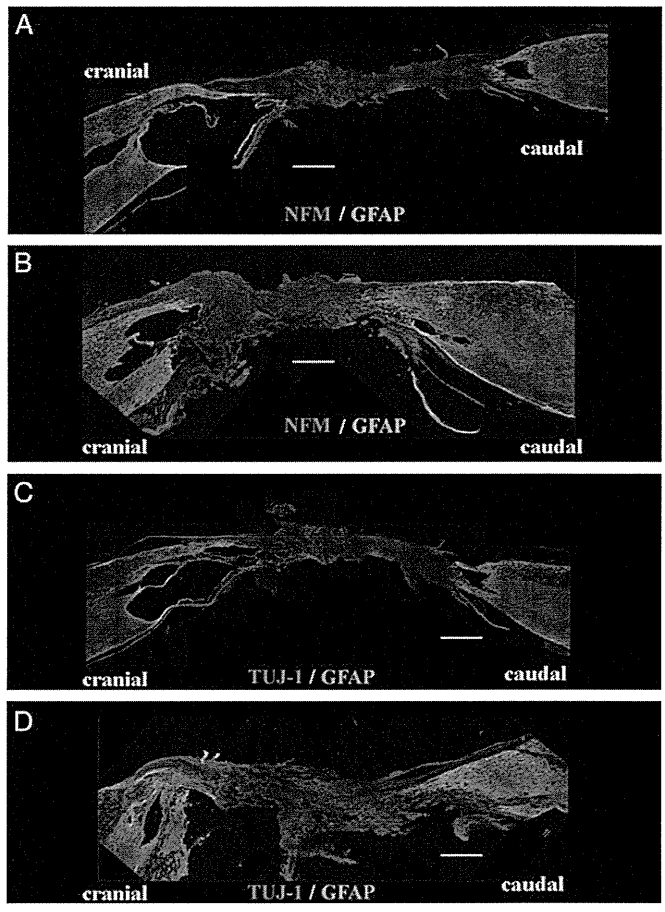

Figure 5. Immunohistochemical appearance of injured transplant site. In SCI controls (*A* to *C*) no NFM or TUJ-1 was noted with only sparse GFAP. Strong NFM and TUJ-1 expression was found in OMT rats (*B* and *D*), implying new axons. GFAP accumulated in injured spinal cord caudal and cranial stumps but was sparse at transplant site. Scale bars represent 500 μm.

connected to Onuf's nucleus, which innervates sphincter motoneurons.[28]

In our study CGRP and GAP43 double positive expression in the L6/S1 dorsal horn in the OMT group was less dense than in SCI controls. This implies that in OMT rats CGRP positive C-fiber afferent sprouting was milder than in SCI controls. Weakened C-fiber sprouting may have attenuated the emergence of urethral excessive bursting and, thus, improved VE in OMT rats. Results may be similar to those in a previous study of transplantation of neuronal and glial precursors for SCI, which suggested decreased CGRP positive C-fiber afferent sprouting and better voiding function than in SCI controls.[24]

How did OMT have a beneficial effect on voiding function after SCI? When looking at the transplant site in the OMT group, NFM and TUJ-1 expression suggests the existence of axons that could not be seen in SCI controls. We cannot state whether these new axons arose from neural stem cells of the transplanted OM or from original axons that regrew from the injured stumps. However, we propose that OMT induced new axons to arise in the injured site and decreased SCI damage, resulting in milder reorganization of the voiding reflex pathway than in SCI controls. We also propose that neurotrophic factor derived from OM components, especially OECs, may modulate voiding reflex reorganization.

The mere existence of new axons in the injured spinal cord may not contribute to functional recovery. However, previous groups reported that after partial SCI intraspinal remodeling occurs cranial and caudal to the injured lesion, resulting in the functional recovery of afferent and efferent pathways.[29,30] If new axons that emerge at the transplant site after OMT serve as interneurons that bridge the injured lesion, this may make it possible to control the urethra and bladder voluntarily according to the descending input from the micturition center in the brain and pons.

In regard to functional analysis in rats with SCI and OMT we are planning neuro-trace or electrophysiological examination from bladder to brainstem (afferent) and from pontine micturition center to bladder (efferent).

A previous clinical study of OMT showed improved motor function and the reemergence of urinary sensation but more than 1 year of rehabilitation after OMT was required until these improvements appeared.[19] Thus, if we study OMT for SCI for a longer period after SCI, we may find more functional voiding recovery. Also, we must investigate OMT for chronic SCI since most patients with SCI have had the injury for several years and the spinal reflex has already reorganized. We may have to study combination therapy, such as OMT with C-fiber desensitization etc, for a better clinical contribution.

CONCLUSIONS

In rats OMT modified the emergence of the spinal micturition reflex after SCI to suppress DSD and it also improved VE. After OMT new axons grew at the transplant site, implying the possible existence of interneurons linking the injured spinal cord to regulate voluntary voiding. If radical therapy for SCI becomes available in the future, urologists will have more opportunity to take part in treatment for voiding dysfunction after SCI.

ACKNOWLEDGMENTS

Dr. Mitsuharu Yoshiyama, Yumura Onsen Hospital, assisted with discussion.

REFERENCES

1. Benevento BT and Sipski ML: Neurogenic bladder, neurogenic bowel, and sexual dysfunction in people with spinal cord injury. Physical Therapy 2002; **82:** 601.

2. Neumann S and Woolf CJ: Regeneration of dorsal column fibers into and beyond the lesion site following adult spinal cord injury. Neuron 1999; **23:** 83.

3. Qiu J, Cai D, Dai H et al: Spinal axon regeneration induced by elevation of cyclic AMP. Neuron 2002; **34:** 895.

4. Morin-Richaud C, Feldblum S and Privat A: Astrocytes and oligodendrocytes reactions after a total section of the rat spinal cord. Brain Res 1998; **783:** 85.

5. Chen MS, Huber AB, van der Haar ME et al: Nogo-A is a myelin-associated neurite outgrowth inhibitor and an antigen for monoclonal antibody IN-1. Nature 2000; **403:** 434.

6. Schwartz M, Lazarov-Spiegler O, Rapalino O et al: Potential repair of rat spinal cord injuries using stimulated homologous macrophages. Neurosurgery 1999; **44:** 1041.

7. Fortun J, Hill CE and Bunge MB: Combinatorial strategies with Schwann cell transplantation to improve repair of the injured spinal cord. Neurosci Lett 2009; **456:** 124.

8. Temeltas G, Dagcid T, Kurt F et al: Bladder function recovery in rats with traumatic spinal cord injury after transplantation of neuronal-glial restricted precursors or bone marrow stromal cells. J Urol 2009; **181:** 2774.

9. Kang SK, Shin MJ, Jung JS et al: Autologous adipose tissue-derived stromal cells for treatment of spinal cord injury. Stem Cells Dev 2006; **15:** 583.

10. Liu S, Qu Y, Stewart TJ et al: Embryonic stem cells differentiate into oligodendrocytes and myelinate in culture and after spinal cord transplantation. Proc Natl Acad Sci U S A 2000; **97:** 6126.

11. Pellitteri R, Spatuzza M, Russo A et al: Olfactory ensheathing cells exert a trophic effect on the hypothalamic neurons in vitro. Neurosci Lett 2007; **417:** 24.

12. O'Toole DA, West AK and Chuah MI: Effect of olfactory ensheathing cells on reactive astrocytes in vitro. Cell Mol Life Sci 2007; **64:** 1303.

13. Teng X, Nagata I, Li HP et al: Regeneration of nigrostriatal dopaminergic axons after transplantation of olfactory ensheathing cells and fibroblasts prevents fibrotic scar formation at the lesion site. J Neurosci Res 2008; **86:** 3140.

14. Lopez-Vales R, Fores J, Navarro X et al: Chronic transplantation of olfactory ensheathing cells promotes partial recovery after complete spinal cord transection in the rat. Glia 2007; **55:** 303.

15. Huard JM, Youngentob SL, Goldstein BJ et al: Adult olfactory epithelium contains multipotent progenitors that give rise to neurons and non-neural cells. J Comp Neurol 1998; **400:** 469.

16. Murrell W, Wetzig A, Donnellan M et al: Olfactory mucosa is a potential source for autologous stem cell therapy for Parkinson's disease. Stem Cells 2008; **26:** 2183.

17. Xiao M, Klueber KM, Lu C et al: Human adult olfactory neural progenitors rescue axotomized rodent rubrospinal neurons and promote functional recovery. Exp Neurol 2005; **194:** 12.

18. Iwatsuki K, Yoshimine T, Kishima H et al: Transplantation of olfactory mucosa following spinal cord injury promotes recovery in rats. Neuroreport 2008; **19:** 1249.

19. Lima C, Pratas-Vital J, Escada P et al: Olfactory mucosa autografts in human spinal cord injury: a pilot clinical study. J Spinal Cord Med 2006; **29:** 191.

20. Gu B, Fraser MO, Thor KB et al: Induction of bladder sphincter dyssynergia by kappa-2 opioid receptor agonists in the female rat. J Urol 2004; **171:** 472.

21. Chien CT, Yu HJ, Lin TB et al: Neural mechanisms of impaired micturition reflex in rats with acute partial bladder outlet obstruction. Neuroscience 2000; **96:** 221.

22. Maggi CA, Giuliani S, Santicioli P et al: Analysis of factors involved in determining urinary bladder voiding cycle in urethane-anesthetized rats. Am J Physiol 1986; **251:** R250.

23. Zinck ND, Rafuse VF and Downie JW: Sprouting of CGRP primary afferents in lumbosacral spinal cord precedes emergence of bladder activity after spinal injury. Exp Neurol 2007; **204:** 777.

24. Mitsui T, Shumsky JS, Lepore AC et al: Transplantation of neuronal and glial restricted precursors into contused spinal cord improves bladder and motor functions, decreases thermal hypersensitivity, and modifies intraspinal circuitry. J Neurosci 2005; **25:** 9624.

25. Fouad K, Pearse DD, Tetzlaff W et al: Transplantation and repair: combined cell implantation and chondroitinase delivery prevents deterioration of bladder function in rats with complete spinal cord injury. Spinal Cord 2009; **47:** 727.

26. Cruz Y and Downie JW: Abdominal muscle activity during voiding in female rats with normal or irritated bladder. Am J Physiol Regul Integr Comp Physiol 2006; **290:** R1436.

27. de Groat WC and Yoshimura N: Mechanisms underlying the recovery of lower urinary tract function following spinal cord injury. Prog Brain Res 2006; **152:** 59.

28. Kakizaki H, Fraser MO and de Groat WC: Reflex pathways controlling urethral striated and smooth muscle function in the male rat. Am J Physiol 1997; **272:** R1647.

29. Bareyre FM, Kerschensteiner M, Raineteau O et al: The injured spinal cord spontaneously forms a new intraspinal circuit in adult rats. Nat Neurosci 2004; **7:** 269.

30. Thuret S, Moon LD and Gage FH: Therapeutic interventions after spinal cord injury. Nat Rev Neurosci 2006; **7:** 628.

Transplantation of olfactory mucosa following spinal cord injury promotes recovery in rats

Koichi Iwatsuki[a], Toshiki Yoshimine[a], Haruhiko Kishima[a], Masanori Aoki[a], Kazuhiro Yoshimura[a], Masahiro Ishihara[a], Yuichiro Ohnishi[a] and Carlos Lima[b]

[a]Department of Neurosurgery, Osaka University Medical School, Suita, Osaka, Japan and [b]Laboratory of Neuropathology, Department of Neurology, Hospital de Egas Moniz, Lisbon, Portugal

Correspondence to Koichi Iwatsuki, MD, Department of Neurosurgery, Osaka University Medical School 2-2 Yamadaoka, Suita, Osaka 565-0871, Japan
Tel: +81 6 6879 3652; fax: +81 6 6879 3659; e-mail: kiwatsuki@nsurg.med.osaka-u.ac.jp

Received 12 March 2008; accepted 20 April 2008

DOI: 10.1097/WNR.0b013e328305b70b

Several recent studies have demonstrated the potential therapeutic role of olfactory ensheathing cells in spinal cord injury. The aim of this study was to elucidate whether grafts of nasal olfactory mucosa containing olfactory ensheathing cells can repair the injured rat spinal cord as compared with the nasal respiratory mucosa containing no olfactory ensheathing cells. These grafts were then transplanted into the partially removed rat spinal cord. Compared with the respiratory mucosa-transplanted rats, the olfactory mucosa-transplanted rats partially recovered the movement of their hindlimbs and joints. Corticospinal tracing indicated that olfactory mucosa transplantation restored the severed tract. Therefore, olfactory mucosa has potential value in the repair of spinal cord injury. *NeuroReport* 19:1249–1252 © 2008 Wolters Kluwer Health | Lippincott Williams & Wilkins.

Keywords: olfactory mucosa, spinal cord injury, transplantation

Introduction

Olfactory ensheathing cells have been studied for their potential in the repair of spinal cord injuries [1–4]. However, in all these experiments, olfactory ensheathing cells were extracted from the olfactory bulb, frequently from the embryo. Consequently, in human spinal therapy, major ethical and technical concerns are associated with the use of embryonic tissues or tissues obtained from the brains of adult donors. These difficulties can be avoided by obtaining the olfactory ensheathing cells from nasal olfactory mucosa.

This study aimed to examine whether grafts of the nasal olfactory mucosa containing olfactory ensheathing cells can repair the injured rat spinal cord as compared with those containing several nonolfactory cell types such as fibroblasts, endothelium, and peripheral nerves and lacking olfactory ensheathing cells. Further, we assessed the functional recovery of the animals using the well-established Basso, Beattie, and Bresnahan Locomotor Rating Scale (BBB scoring system) [5]. Immunohistochemistry was performed to provide anatomical evidence of olfactory ensheathing cells in the grafted site, and anterograde corticospinal tract tracing study was carried out to document the regrowth of axons.

Materials and methods

Spinal cord injury

Female Sprague–Dawley rats weighing 250–300 g were anesthetized using a ketamine/rompun mixture (90/10 mg/kg, intraperitoneally). The rectal temperature was maintained at 37±0.5°C with a heating pad. The skin and the muscles of the back were incised to expose the thoracic (Th) 8–9 vertebrae. A laminectomy was performed at Th 8–9 using a microsurgery bone rongeur, and the spinal cord was exposed without touching it. A 1.5-mm gap was created by excision of a 1.5-mm region of the spinal cord using microscissors.

Dissection and preparation of the olfactory and respiratory mucosa

Adult Sprague–Dawley rats were deeply anesthetized using sodium pentobarbital (100 mg/kg) and sacrificed by decapitation. The nasal septum was freed by removing the lower jaw, upper teeth, and nasal turbinates. Both olfactory and respiratory mucosae were identified on the septum.

The olfactory mucosa was located in its dorsocaudal portion and is easily identifiable by the yellowish appearance of its surface. The respiratory mucosa was located ventrorostral to the olfactory mucosa and identified by the grayish color of its surface. Each mucosa was dissected carefully to exclude the border region between the mucosae to avoid contamination.

Transplantation of the olfactory and respiratory mucosa

Before transplantation, both mucosae were cut into approximately 0.5-mm to 1.0-mm sections. Next, four to six sections of the olfactory and respiratory mucosa were gently inserted into the cavity made in the spinal cord to fill it. Seven animals received transplants of the olfactory mucosa and

seven control animals received transplants of the respiratory mucosa. The wound was sealed by suturing the muscle and the skin overlaying the exposed spine.

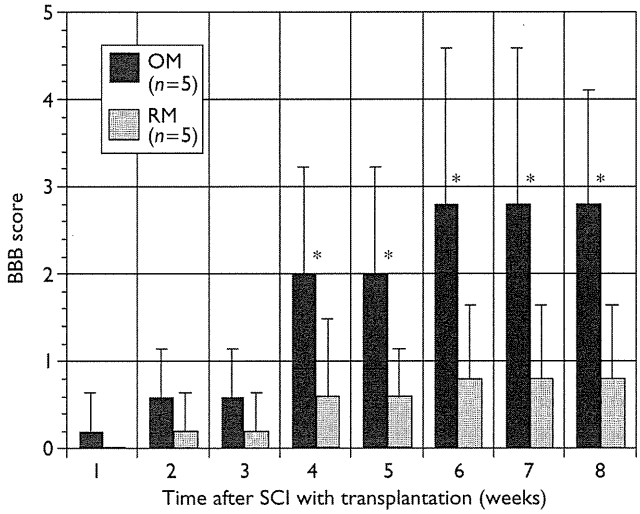

Fig. 1 A statistically significant greater functional recovery in hindlimb usage was observed in the olfactory mucosa-transplanted rats (OM) as compared with the respiratory mucosa-transplanted rats (RM) 4 weeks after the transplantation (*). BBB, Basso, Beattie, and Bresnahan Locomotor Rating Scale.

Behavioral assessment

The BBB score is an operationally defined 21-point scale. It is designed to assess the hindlimb locomotor recovery after impact injury to the thoracic cord in rats [5]. These BBB scores were determined by two observers, who were blinded to this study, and the scores were averaged and compared between the olfactory and respiratory mucosa-transplanted groups using the Student's *t*-test for these unpaired results. Statistical significance was set at $P<0.05$.

Histological assessment

The animals were transcardially perfused with 100 ml of 4% paraformaldehyde in 0.2 M phosphate-buffered saline (PBS), followed by perfusion with 20 ml of PBS. The spinal cord encompassing the transplantation site was removed, post fixed for 2 h in the same fixative, cryoprotected in 30% sucrose, and prepared for cryosectioning. The spinal cord was sectioned longitudinally and 20-μm thick sections were obtained. After blocking with 5% normal goat serum and 0.3% Triton-X in PBS, the sections were incubated with a primary antibody to a mouse monoclonal antibody raised against p75NGFR [Chemicon, Temecula, California, USA, Cat. No. MAB365; dilution, 1 : 500 in 0.1 M PBS (pH 7.4)] and glial fibrillary acidic protein (dilution, 1 : 100; cow polyclonal antibody; Dako, Produktionsveg, Glostrup, Denmark). On the following day, sections were washed with PBS and incubated for 20 min in secondary antibody [goat anti-mouse IgG (H+L); Alexa 488 molecular probes,

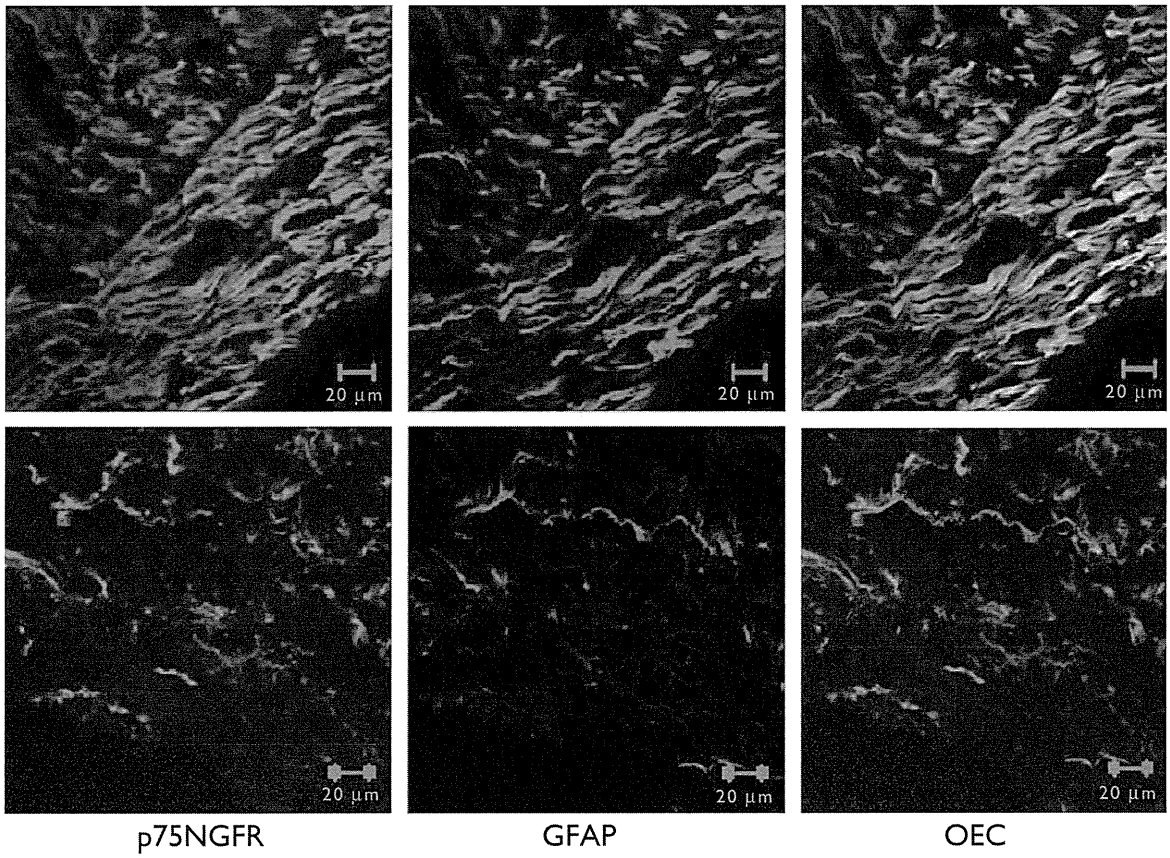

Fig. 2 Strong expression of p75NGFR (upper left) and GFAP (upper middle) of p75NGFR is observed in the olfactory mucosa graft at 2 weeks after transplantation; however, expression of p75NGFR (lower left) and GFAP (lower middle) is weak in the olfactory mucosa graft at 8 weeks after the transplantation. The p75NGFR merged with the GFAP is OEC. The expression of OEC is strong at 2 weeks after the transplantation (upper right) and weak at 8 weeks after the transplantation (lower right). GFAP, glial fibrillary acidic protein.

No. A-11029]. The sections were fixed in Crystal/Mount (Biomeda, Foster, California, USA) and observed under a confocal laser microscope (Zeiss, Berlin, Germany, LSM-510 META/UV). Olfactory ensheathing cells are known to express markers typical to the nonmyelin-forming Schwann cell phenotype, namely, low-affinity p75NGFR [6].

Anterograde tracing

Eight weeks after the spinal cord surgery, four rats (two each from the olfactory and respiratory mucosa-transplanted groups) were anesthetized by ketamine (70 mg/kg) and xylazine (8 mg/kg). The cranial bone overlying the motor cortex was removed.

Electrophysiological recording of hindlimb movement was used to confirm the injection site (1–3 mm posterior to bregma and 1–3 mm lateral to bregma). Eight injections (four on each side) of 10% fluorescence-labeled biotinylated dextran amine (BDA) (Molecular Probes, BDA-10 000; Invitrogen, Carlsbad, California, USA) were done bilaterally into the motor cortex with a microsyringe (8 × 0.5 μl). Two weeks after the BDA injection, the rats were perfused with 4% paraformaldehyde in 0.1 M phosphate buffer (pH 7.4). The spinal cords were collected and longitudinally sliced into 20-μm thick sections on a freezing microtome. The sections were examined under a fluorescence microscope.

All experimental protocols and procedures for this study were approved by the Animal Ethics Committee of the Osaka University.

Results

Autophagia was only observed in two animals in each group. These animals were euthanized 3 days post operatively and were excluded from the analysis of this study. A greater functional recovery in the hindlimb usage was observed in the olfactory mucosa-transplanted rats (n=5) as compared with the control rats (n=5) (Fig. 1). The recovery of hindlimb movement was measurable by 4 weeks after the transplantation in the olfactory mucosa-transplanted rats, with continued divergence of the mean BBB scores until 6 weeks after the transplantation (Fig. 1).

The expression of p75NGFR was strong in the grafts at 2 weeks after the olfactory mucosa transplantation; however, it was weak in the grafts at 8 weeks after the transplantation (Fig. 2).

BDA-labeled fibers were clearly observed in the rostral segment of the graft from olfactory mucosa (Fig. 3a and b), but they were scarcely present in the caudal segment (Fig. 3a and c). No apparent behavioral recovery (BBB score 0–2) or BDA-labeled fibers were observed in the caudal segment of the graft from respiratory mucosa. No p75NGFR positive nuclei were present in the control rats with grafts from respiratory mucosa.

Discussion

Olfactory ensheathing cells expressing p75NGFR were strongly detected in the graft at 2 weeks after transplanta-

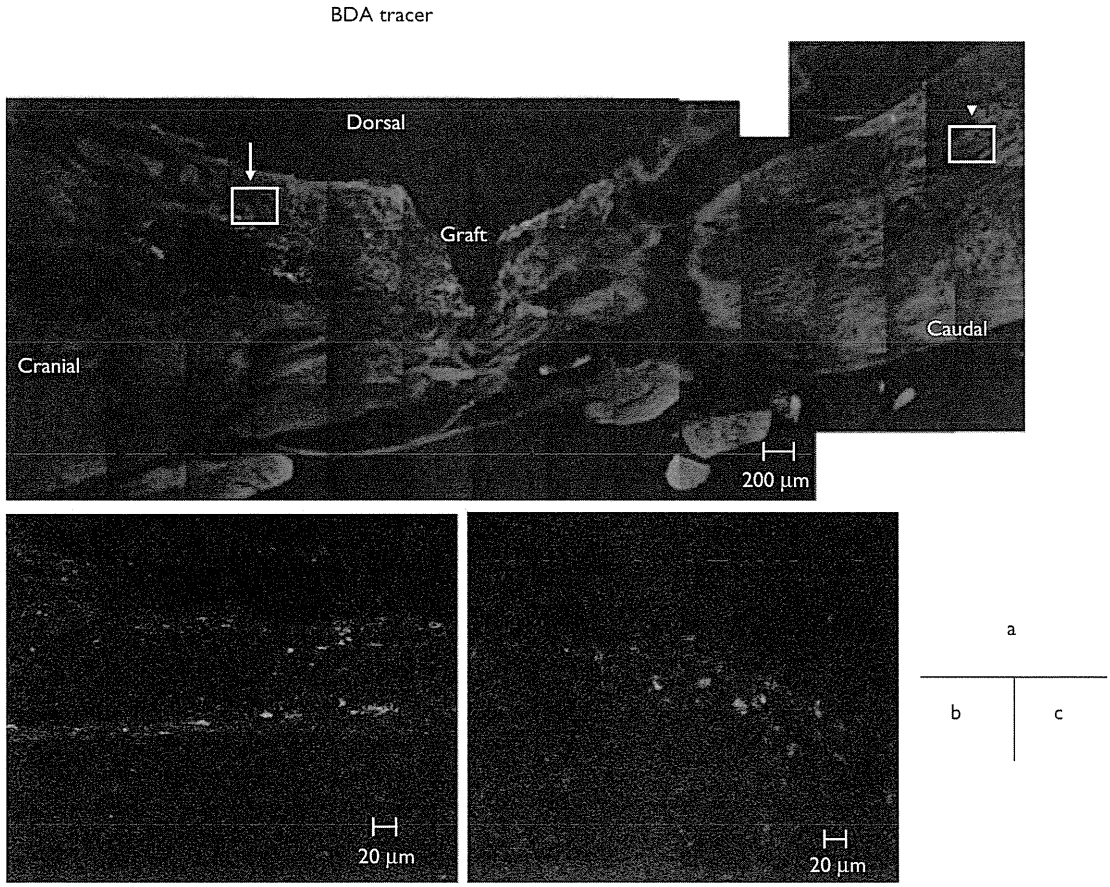

Fig. 3 Corticospinal tract study using BDA (a). BDA-labeled fibers were clearly observed in the rostral segment of the olfactory mucosa-transplanted graft [(a). arrow, (b)] and slightly present in the caudal segment [(a), arrowhead, (c)].

tion. Ensheathing cells are specialized glial cells that associate with the olfactory nerve, surrounding the sensory axons as they leave the olfactory epithelium and accompanying them from the nose to the brain where they synapse with the mitral cells of the olfactory bulb [7]. Two properties of ensheathing cells render them unique. First, ensheathing cells exist both outside and inside the central nervous system (such as Schwann cells and astrocytes, respectively). The second unique property arises from the fact that a continual neurogenesis occurs within the olfactory epithelium, which produces new sensory neurons throughout adult life. This property is also observed in ensheathing cells in humans [8]. The ensheathing cells do not normally myelinate the olfactory nerve. However, they appear to myelinate the regrowing axons in the region of injury after corticospinal lesions [9], and they remyelinate axons in several demyelinating models [10,11] when transplanted into the spinal cord. This neurogenesis is a highly regulated process, which is assisted by olfactory ensheathing cells, although the specific role of these cells remains unclear. A crucial property of ensheathing cells is their superior ability to interact with astrocytes. When the superficial astrocytic processes, which form the glial scar after lesions, come into contact with ensheathing cells, the astrocytic processes change their configuration so that the glial pathway for axonal regeneration is formed. Thus, the glial pathway enables axonal regeneration [12]. This renders the ensheathing cell an attractive subject for transplantation into spinal cord lesions. Even at the short survival periods examined in this study, the rate of functional recovery following olfactory mucosa transplantation was better than that after respiratory mucosa transplantation. Further, in our study, p75NGFR expression was strong in the grafts at 2 weeks after the transplantation; however, it was weak in the grafts at 8 weeks after the transplantation (Fig. 3). This might indicate that the axonal regeneration was activated at 2 weeks and decreased at 8 weeks after the transplantation. There are many other advantages of using olfactory tissue. First, it would allow autologous transplantation; second, it would provide a cellular bridge that would join the gap between the transected ends of the spinal cord, thus avoiding the need for an artificial bridge; and third, this tissue can be obtained by a simple biopsy that is performed through the external nares [13].

Conclusion

Transplantation of the nasal olfactory mucosa promotes partially functional and structural restoration of the severed corticospinal tract. The autologous procurement of mucosa via the external nares is a less invasive and a practical approach for the treatment of spinal cord injury.

References

1. Barnett SC, Alexander CL, Iwashita Y, Gilson JM, Crowther J, Clark L, *et al.* Identification of a human olfactory ensheathing cell that can effect transplant-mediated remyelination of demyelinated CNS axons. *Brain* 2000; **123**:1581–1588.
2. Smith PM, Lakato SA, Barnett SC, Jeffery ND, Franklin RJM. Cryopreserved cells isolated from the adult canine olfactory bulb are capable of extensive remyelination following transplantation into the adult rat CNS. *Exp Neurol* 2002; **176**:402–406.
3. Li Y, Carlstedt T, Berthold CH, Raisman G. Interaction of transplanted olfactory-ensheathing cells and host astrocytic processes provides a bridge for axons to regenerate across the dorsal root entry zone. *Exp Neurol* 2004; **188**:300–308.
4. Ramon-Cueto A, Cordero MI, Santos-Benito FF, Avila J. Functional recovery of paraplegic rats and motor axon regeneration in their spinal cords by olfactory ensheathing glia. *Neuron* 2000; **25**:425–435.
5. Basso DM, Beattie MS, Bresnahan JC. A sensitive and reliable locomotor rating scale for open field testing in rats. *J Neurotrauma* 1995; **12**:1–21.
6. Ramon-Cueto A, Plant GW, Avila J, Bunge MB. Long-distance axonal regeneration in the transected adult rat spinal cord is promoted by olfactory ensheathing glia transplants. *J Neurosci* 1998; **18**:3803–3815.
7. Doucette R. Glial cells in the nerve fiber layer of the main olfactory bulb of embryonic and adult mammals. *Microsc Res Tech* 1993; **24**:113–130.
8. Murrell W, Bushell GR, Livesey J, McGrath J, MacDonald KP, Bates PR, *et al.* Neurogenesis in adult human. *Neuroreport* 1996; **7**:1189–1194.
9. Li Y, Field PM, Raisman G. Regeneration of adult rat corticospinal axons induced by transplanted olfactory ensheathing cells. *J Neurosci* 1998; **18**:10514–10524.
10. Franklin RJ, Gilson JM, Franceschini IA, Barnett SC. Schwann cell-like myelination following transplantation of an olfactory bulb-ensheathing cell line into areas of demyelination in the adult CNS. *Glia* 1996; **17**:217–224.
11. Radtke C, Akiyama Y, Brokaw J, Lankford KL, Wewetzer K, Fodor WL, *et al.* Remyelination of the nonhuman primate spinal cord by transplantation of H-transferase transgenic adult pig olfactory ensheathing cells. *FASEB J* 2004; **18**:335–337.
12. Ying LI, Daqing LI, Raisman G. Interaction of olfactory ensheathing cells with astrocytes may be the key to repair of tract injuries in the spinal cord: the 'pathway hypothesis'. *J Neurocytol* 2005; **34**:343–351.
13. Feron F, Perry C, McGrath JJ, Mackay-Sim A. New techniques for biopsy and culture of human olfactory epithelial neurons. *Arch Otolaryngol Head Neck Surg* 1998; **124**:861–866.

Phytomedicine 21 (2014) 247–253

Contents lists available at ScienceDirect

Phytomedicine

journal homepage: www.elsevier.de/phymed

Mallotus philippinensis bark extracts promote preferential migration of mesenchymal stem cells and improve wound healing in mice

Tadashi Furumoto[a], Noriyasu Ozawa[a,b], Yuta Inami[a,b], Misaki Toyoshima[a,b], Kosuke Fujita[a,b], Kaori Zaiki[a,b], Shunya Sahara[a,b], Mariko Akita[a,b], Keiko Kitamura[a,b], Koichi Nakaoji[a,b], Kazuhiko Hamada[b], Katsuto Tamai[c], Yasufumi Kaneda[d], Akito Maeda[a,*]

[a] *Skin Regeneration, PIAS Collaborative Research, UIC, Osaka University, Japan*
[b] *Research & Development Division, PIAS Corporation, Japan*
[c] *Division of Stem Cell Therapy Science, Graduate School of Medicine, Osaka University, Japan*
[d] *Division of Gene Therapy Science, Graduate School of Medicine, Osaka University, Japan*

ARTICLE INFO

Article history:
Received 22 July 2013
Accepted 19 September 2013

Keywords:
Phenolic compounds
Mallotus philippinensis
Mesenchymal stem cells
Migration
Wound healing

ABSTRACT

In the present study, we report the effects of the ethanol extract from *Mallotus philippinensis* bark (EMPB) on mesenchymal stem cell (MSC) proliferation, migration, and wound healing *in vitro* and in a mouse model. Chemotaxis assays demonstrated that EMPB acted an MSC chemoattractant and that the main chemotactic activity of EMPB may be due to the effects of cinnamtannin B-1. Flow cytometric analysis of peripheral blood mononuclear cells in EMPB-injected mice indicated that EMPB enhanced the mobilization of endogenous MSCs into blood circulation. Bioluminescent whole-animal imaging of luciferase-expressing MSCs revealed that EMPB augmented the homing of MSCs to wounds. In addition, the efficacy of EMPB on migration of MSCs was higher than that of other skin cell types, and EMPB treatment improved of wound healing in a diabetic mouse model. The histopathological characteristics demonstrated that the effects of EMPB treatment resembled MSC-induced tissue repair. Taken together, these results suggested that EMPB activated the mobilization and homing of MSCs to wounds and that enhancement of MSC migration may improve wound healing.

Introduction

Mesenchymal stem cells (MSCs) are capable of differentiating into various cells and secrete numerous pro-regenerative factors, thereby enabling the regeneration of damaged tissue (Phinney and Prockop 2007). MSCs are found in the bone marrow or perivascular regions of blood vessels (Crisan et al. 2008) and express Sca-1 and platelet-derived growth factor receptor (PDGFR) α on the cell surface (Morikawa et al. 2009). Several studies have indicated that MSCs migrate to the wound site during wound healing (Fathke et al. 2004; Sasaki et al. 2008). MSCs are used as cell therapy for several diseases because they can be easily isolated (Vojtassak et al. 2006). Therefore, methods for enhancing the mobilization and homing of MSCs to wounds have the potential to improve the effectiveness of wound healing.

Mallotus philippinensis Muell-Arg (Euphorbiaceae) has been widely used in traditional medicine (Sharma and Varma 2011). In a preliminary screening experiment, the ethanol extract of *M. philippinensis* bark (EMPB) was found to activate MSC migration *in vitro* (Furumoto et al., unpublished data). In the present study, we characterized the migratory activity of MSCs after EMPB treatment and examined the effects of EMPB on wound healing in mice in order to identify novel EMPB components with the ability to enhance MSC migration.

Materials and methods

Preparation of the extract

M. philippinensis from Nepal was purchased from MARUZEN PHARMACEUTICALS Ltd. (Hiroshima, Japan). Chopped bark from *M. philippinensis* was extracted for 2 h with aqueous ethanol (80%, v/v) by reflux extraction. The isolated extract was adjusted to have an ethanol concentration of 50% v/v, dried, and collected as a powder of EMPB.

* Corresponding author at: Skin Regeneration, PIAS Collaborative Research, UIC, Osaka University, 2-1 Yamada-oka, Suita 565-0871, Japan. Tel.: +81 6 6816 8456; fax: +81 6 6816 8460.
E-mail address: amaeda@uic.osaka-u.ac.jp (A. Maeda).

0944-7113/$ – see front matter © 2013 Elsevier GmbH. All rights reserved.
http://dx.doi.org/10.1016/j.phymed.2013.09.003

HPLC fingerprint analysis

Separation of the extract was performed using the Wakosil-II 5C18HG HPLC column (Wako, Japan) in 0.172% phosphoric acid containing 12.5% acetonitrile and 1.5% tetrahydrofuran. The flow rate was 1 ml/min at 40 °C, and detection was carried out at 280 nm. LC–MS was performed using the Xevo G2 Tof system (Waters, Milford, USA). The mobile phase consisted of solvent A (0.1% formic acid/H_2O) and solvent B (0.1% formic acid/MeCN). Gradient elution was performed (0–1 min A:B, 90:10; 1–8 min A:B, 90:10 → 0:100; 8–9 min A:B, 0:100; and 9–10 min A:B, 90:10) at a flow rate of 0.4 ml/min. Mass spectrometry was performed in the negative ion mode. The NMR values of cinnamtannin B-1 in peak 3 were analyzed as described previously (Kamiyama et al. 2001).

In vitro assays

KUM6 cells were provided by the RIKEN, Japan. NIH-3T3 and RAW264.7 cells were cultured in DMEM containing 10% FBS and 2 mM L-glutamine. Normal human epidermal keratinocytes (NHEKs) were purchased from KURABO Industries Ltd. (Osaka, Japan). Maintenance of human aortic endothelial cells (HAECs), proliferation assay, migration assay, and real-time PCR with primers of type I collagen were carried out as described previously (Nishikawa et al. 2009).

In vivo experiments

Mice were obtained from Clea Japan (Osaka, Japan). All experimental protocols were approved by the Osaka University Graduate School of Medicine Standing Committee on Animals. In MSC mobilization assay, nucleated cells in blood were analyzed as described previously (Tamai et al. 2011). In MSC homing assay, full-thickness wounds (0.8 cm in diameter) were created and AteloCell (Koken Co. Ltd., Tokyo, Japan) containing EMPB was topically applied. At 4 days post surgery (day 0), 2.5×10^5 KUM6 cells transiently transfected with an expression vector for firefly luciferase, pGL4.50 (Promega, USA) were injected into the tail veins of mice. Bioluminescence was measured as described previously (Battula et al. 2010). In the wound healing model, full-thickness wounds (1.5 cm in diameter) were made as previously described (Greenhalgh et al. 1990). EMPB was topically applied 3 times per week. Serial sections from the wound were evaluated with H&E staining, α-smooth muscle actin (α-SMA; DAKO, Glostrup, Denmark) immunostaining, and Masson Trichrome staining.

Statistical analysis

Results are expressed as means ± SE. Statistically significant differences between control and other groups were determined using the Dunnett's test. * and ** corresponded to $p < 0.05$ and $p < 0.01$, respectively.

Results

HPLC fingerprint analysis of EMPB

HPLC profiles of EMPB (Fig. 1) showed that EMPB consists of 3 compounds eluting with different retention times. The individual compounds were further characterized by LC/MS and identified as protocatechuic acid (peak 1, 5.788 min), salicylic acid (peak 2, 7.676 min), and cinnamtannin B-1 (peak 3, 12.817 min). In terms of abundance, peaks 1, 2, and 3 accounted for 52%, 17%, and 31% of total EMPB composition, respectively. LC/MS signals for condensed tannins were also observed in minor peaks.

Effects of EMPB on MSC proliferation and migration

We examined the effect of EMPB and its constituents on the proliferation of mouse MSC cells KUM6 (Umezawa et al. 1992) by MTS assays, and on the migration of KUM6 cells by Boyden chamber migration assay. The proliferation of KUM6 cells was enhanced in EMPB (0.16–4 μg/ml) (Fig. 2A), whereas EMPB was toxic at 20 μg/ml. The migratory activity of KUM6 cells increased with 0.8–4 μg/ml EMPB, as compared with the control (Fig. 2B). Cinnamtannin B-1 promoted the proliferation and migration of KUM6 cells when used at concentrations of 0.16–20 μg/ml and 0.8–4 μg/ml, respectively (Fig. 2C and D), whereas protocatechuic acid caused only a slight increase in the proliferation at high concentrations (Fig. 2E and F). Salicylic acid did not affect either proliferation or migration under comparable conditions (Fig. 2G and H). These results strongly suggest that EMPB enhances the proliferation and

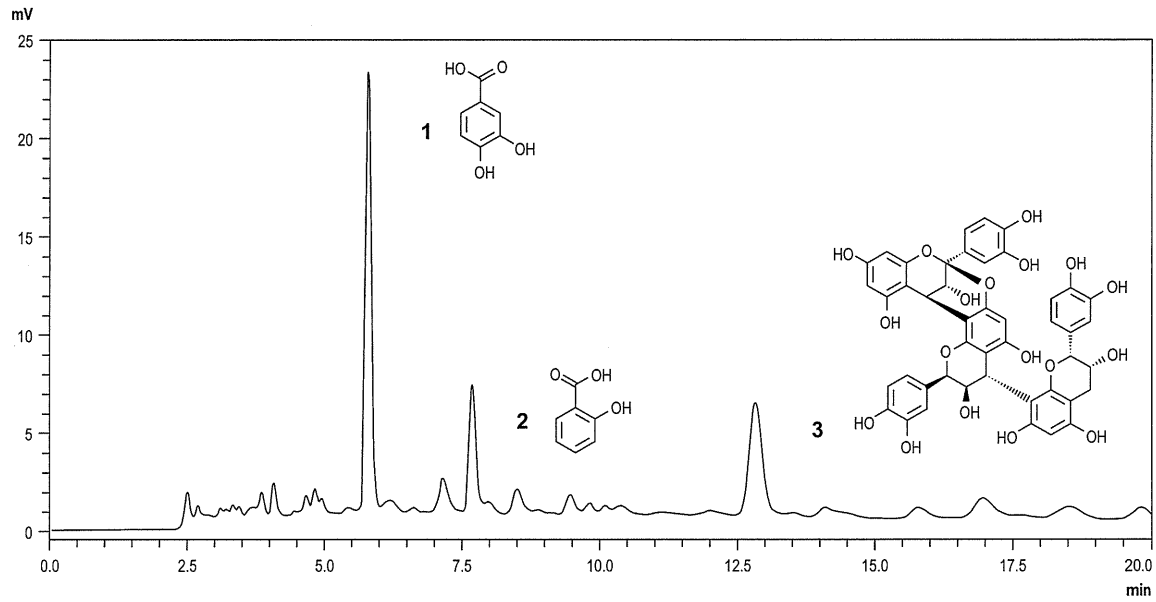

Fig. 1. HPLC analysis of EMPB composition.

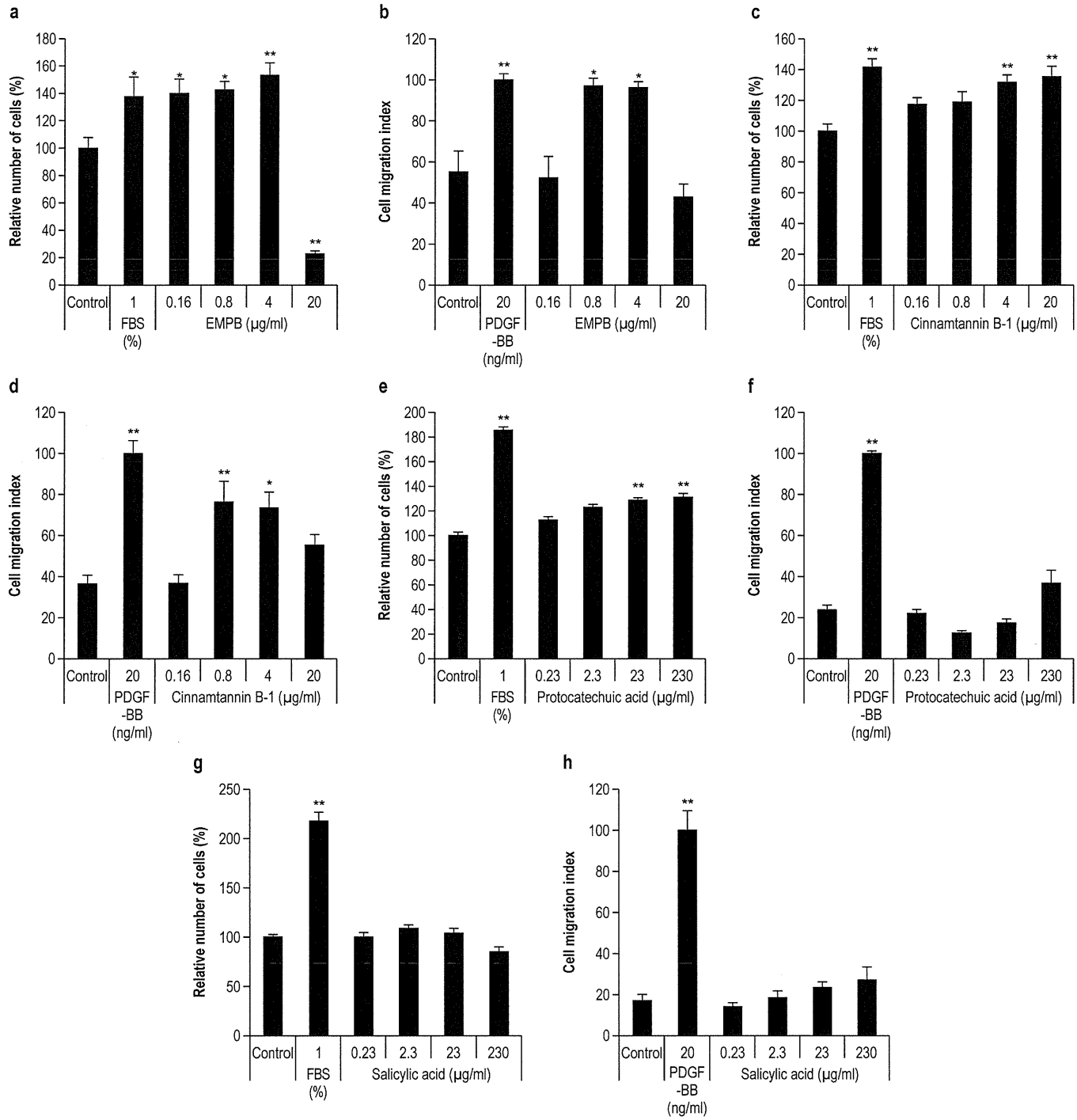

Fig. 2. Effects of EMPB on KUM6. (A) KUM6 cell proliferation. Values are expressed as mean (±SE) percentages normalized to untreated controls. $n = 4$. (B) KUM6 cell migration. Values are expressed as mean (±SE) migration indices normalized to positive control. $n = 4$. (C, E, and G) KUM6 cell proliferation after stimulation with cinnamtannin B-1, protocatechuic acid, and salicylic acid, respectively. (D, F, and H) KUM6 cell migration after stimulation with cinnamtannin B-1, protochatechuic acid, and salicylic acid, respectively.

migration of KUM6 cells *in vitro* and the main activity of EMPB is mediated by cinnamtannin B-1.

Enhancement of the MSC migratory capacity by EMPB treatment in vivo

Recent studies have shown that the PDGFRα-positive non-hematopoietic cell population in blood circulation after tissue injury contains MSCs (Tamai et al. 2011). Therefore, to investigate the influence of EMPB on the mobilization of endogenous MSCs, we analyzed the number of MSCs in the blood circulation 1 h after injecting 2.16 mg/kg EMPB (a nontoxic concentration) into C57BL/6NJcl mice. Flow cytometric analysis indicated that the population of lineage-negative PDGFRα$^+$ and Sca-1$^+$ (Lin$^-$/PDGFRα$^+$/Sca-1$^+$) cells was increased in EMPB-treated mice as compared with control mice (Fig. 3A). These results indicated that EMPB enhanced the mobilization of endogenous MSCs into the blood circulation.

We further examined whether EMPB could also upregulate the ability of MSCs to home to wounded sites. We injected MSCs

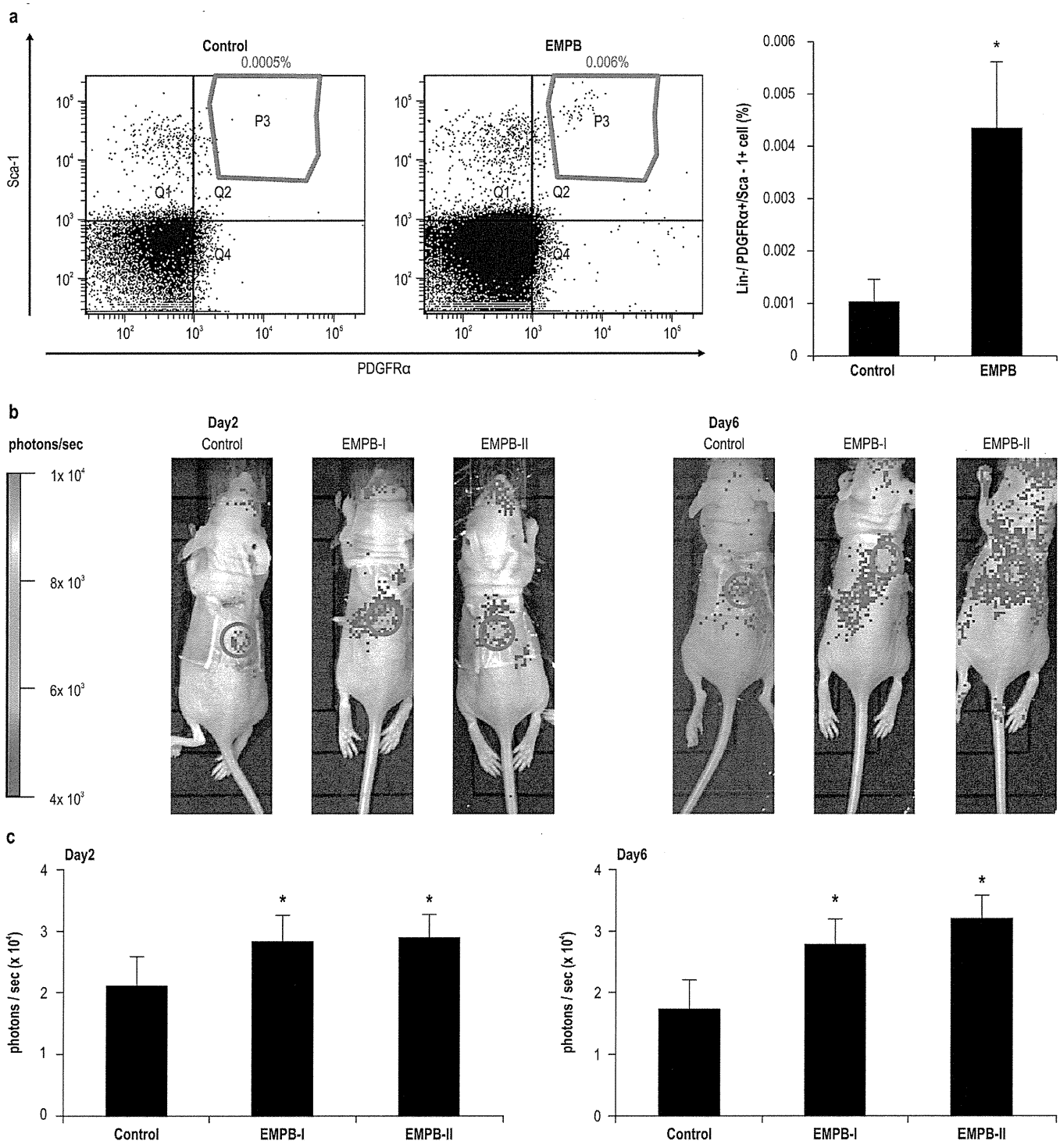

Fig. 3. Effects of EMPB on the migratory capacity of MSCs in mice. (A) Flow cytometric analyses of $Lin^-/PDGFR\alpha^+/Sca\text{-}1^+$ (gated) peripheral blood mononuclear cells of mice after systemic administration of EMPB. $n = 4$. (B) ffLuc-expressing KUM6 colocalization in wound healing models. (C) Quantification of the photon counts at the wound site. $n = 3–5$.

transiently expressing firefly luciferase (ffluc) into the tail veins of BALB/cAJcl-nu/nu mice bearing dorsal wounds covered with a collagen sponge containing EMPB (group I: 2 μg; group II: 6 μg) and detected bioluminescence by whole-animal imaging. Interestingly, ffluc-expressing MSCs were increased in the wounded regions after 2 and 6 days (Fig. 3B). The photon counts at the wound site were 1.5–2-fold higher in EMPB treated mice relative to control mice (Fig. 3C). These results indicate that EMPB also enhanced the homing of MSCs from systemic circulation to the wound site.

Effects of EMPB on the proliferation and migration of fibroblasts, keratinocytes, macrophages, and vascular endothelial cells

Next, we examined the effects of EMPB on the proliferation and migration of fibroblasts, keratinocytes, macrophages, and vascular endothelial cells, which are commonly found in skin tissues. EMPB promoted the proliferation and migration of NIH3T3 fibroblasts when used at concentrations of 0.16–20 μg/ml and 4–20 μg/ml, respectively (Fig. 4A and B), whereas EMPB did not affect collagen

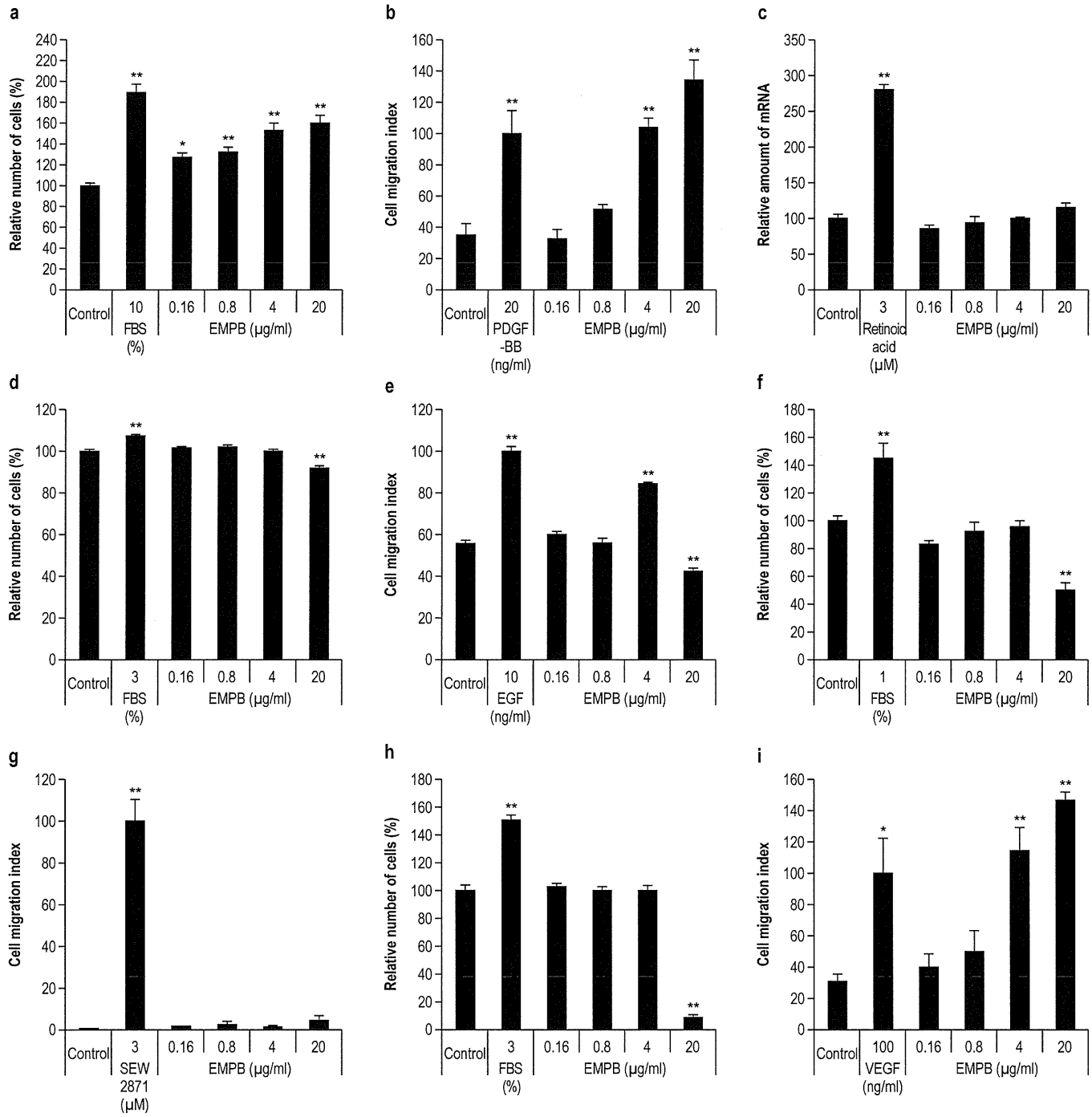

Fig. 4. Effects of EMPB on fibroblasts, keratinocytes, macrophages, and vascular endothelial cells. (A) NIH3T3 cell proliferation ($n=4$). (B) NIH3T3 cell migration ($n=4$). (C) Collagen production in NIH3T3 cells. (D) NHEK cell proliferation. (E) NHEK cell migration. (F) RAW264.7 cell proliferation. (G) RAW264.7 cell migration. (H) HAEC cell proliferation. (I) HAEC cell migration.

production in NIH3T3 cells, as determined by real-time PCR (Fig. 4C). The migration of NHEKs was slightly increased with 4 μg/ml EMPB (Fig. 4E). However, EMPB had no significant effect on the proliferation of NHEKs (Fig. 4D) or RAW264.7 macrophages (Fig. 4F) or on the migration of RAW264.7 macrophages (Fig. 4G). Additionally, the migration, but not proliferation, of HAECs was increased by application of 4–20 μg/ml EMPB (Fig. 4I and H). These results indicate that the effects of EMPB may be cell-type specific. The maximum efficacy dose of EMPB on the migration of KUM6 cells was lower (0.8 μg/ml) than that of NIH3T3 cells, NHEKs, and HAECs in the migration assay. These data indicate that the efficacy of EMPB on the migration of MSCs is higher than its efficacy on the migration of other cell types.

Effects of EMPB treatment on wound healing in mice

The effects of EMPB on wound healing were analyzed in the diabetic mouse model C57BLKS/JIar- + $Lepr^{db}$/ + $Lepr^{db}$. Application of 1.3 μg/wound EMPB (EMPB-II) resulted in a significant reduction in the wound area from days 7 to 17 as compared to application of PBS alone as control (Fig. 5A and B). A slight reduction in the wound

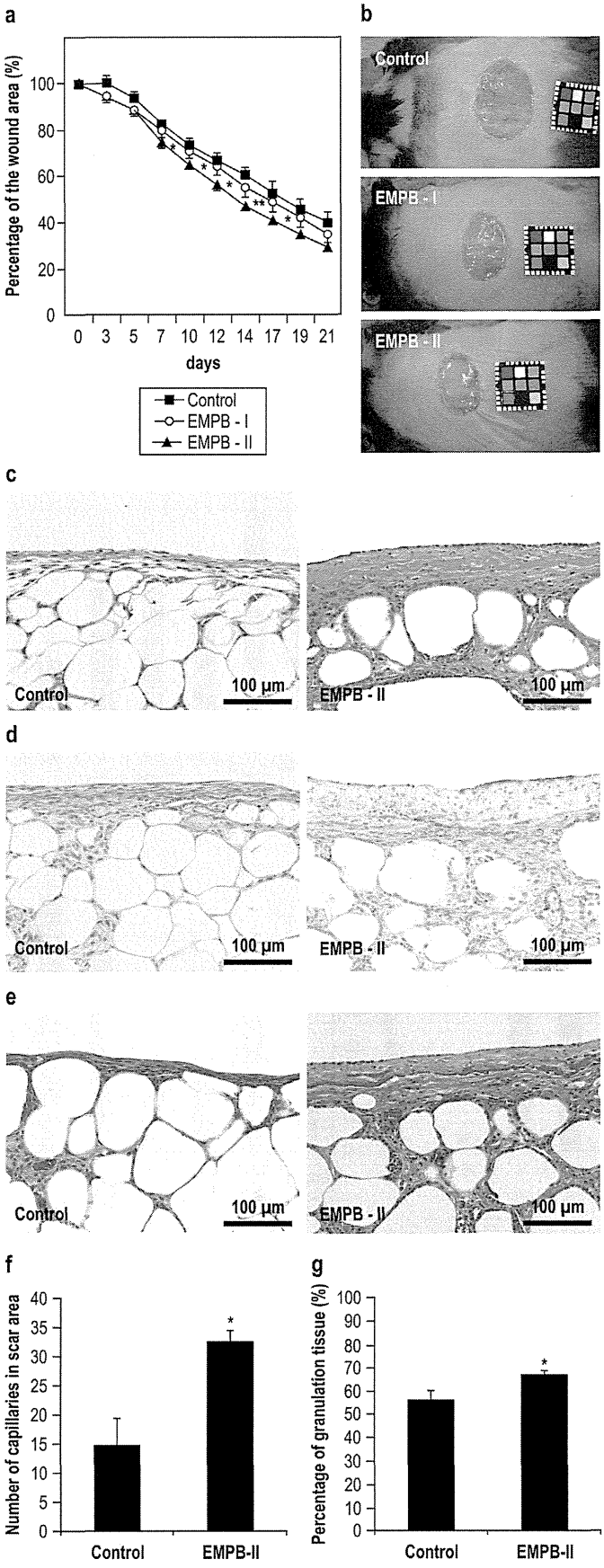

Fig. 5. Effects of EMPB in a diabetic mouse wound healing model. (A) Time course of the quantification of wound size. The percent of the wound area (%) was calculated as the wound area at different times/wound area at day 0 × 100 ($n = 10$). (B) Representative images of wounds on day 14. (C) H&E staining of the specimens on day 10 (200×). (D) α-SMA immunostaining (200×). (E) Masson Trichrome staining (200×). (F) The number of capillaries in the scar area was counted ($n = 6$). (G) The percentage of granulation tissue (%) was calculated as the blue stained portion/the entire scarred area × 100 ($n = 6$).

area was also observed in mice treated with 0.4 μg/wound EMPB (EMPB-I).

Several reports have indicated that MSCs enhance wound closure, granulation tissue formation, collagen production, and angiogenesis during tissue repair (Wu et al. 2010). Therefore, we further examined the effects of EMPB on tissue regeneration. Randomly selected photographs of wound tissue on day 10 from mice in EMPB-II are shown in Fig. 5C. In general, the epithelialization and the formation of granulation tissues was not obvious in control animals, but was highly significant in EMPB-II-treated mice. These data imply that EMPB improves wound healing by facilitating tissue regeneration. Next, we compared angiogenesis in the wound area, by analyzing the number of capillaries stained with α-SMA in the entire granulation area. EMPB-II exhibited significant increases in the number of capillaries formed as compared to control (Fig. 5D and F). Masson Trichrome staining also showed a significant increase in granulation tissue content in EMPB-II-treated mice (Fig. 5E and G). These results suggest that EMPB may accelerate tissue regeneration during the wound healing process and that the characteristics of tissue regeneration may resemble MSC-induced tissue repair.

Discussion

MSCs are thought to play an important role in tissue regeneration following organ injury (Phinney and Prockop 2007), and therapeutic approaches to directly target MSCs have been investigated in various animal models. As strategies in these models, transgenic approaches, priming, enhancing endogenous mechanisms of homing, and targeting using tissue-specific cues have been reported (Wagner et al. 2009). We demonstrated that the components of EMPB also had the potential to act as a chemical enhancer of MSC migration. These data suggest that the components of *M. philippinensis* may provide new therapeutic options for regenerative medicine.

In this study, we observed an increase in the $Lin^-/PDGFR\alpha^+/Sca\text{-}1^+$ cell population in the blood circulation with EMPB treatment because EMPB induced MSC mobilization. Similar to chemotaxis induced by cytokines (Tamai et al. 2011), EMPB seems to attract MSCs from the bone marrow or perivascular regions into blood circulation. Moreover, *in vivo* wound homing assays in nude mice revealed that EMPB could induce dynamic changes in MSCs around dorsal wounds. In this context, EMPB may direct the homing of MSCs from blood circulation to the wound region. These data suggest that EMPB may mediate multiple functions in the migration of MSCs. *In vitro* cell migration assays revealed that the main activity of EMPB in chemotaxis may be facilitated by cinnamtannin B-1 and that components of EMPB may directly activate the migration of MSCs. Therefore, we speculate that cinnamtannin B-1 directly activates cell migration-associated signal transduction, which is functional in MSCs. Additionally, cinnamtannin B-1 has been shown to exhibit antioxidant and antimicrobial activities (Idowu et al. 2010); thus, it is expected to have protective effects on damaged tissues. Our future studies will focus on the identification of migration-associated signaling pathways mediated by the active components of EMPB in MSCs.

Our data confirmed that EMPB contains protocatechuic acid. Protocatechuic acid has been shown to promote the migration and proliferation of adipose tissue-derived stromal cells (ADSCs) *in vitro* (Wang et al. 2008, 2009). ADSCs found in the subcutaneous adipose

tissue have the potential to differentiate into mesodermal cells. This implies that the components of EMPB not only affect MSC mobilization and homing, but may also induce other effects, thereby assisting in wound healing.

Our results in a diabetic mouse model of wound healing showed that EMPB accelerated wound repair. Histopathological analysis after EMPB treatment indicated that the increased epithelialization activity, angiogenesis, granulation tissue formation, and remodeling in the wound healing process may result in a significant reduction in wound size. MSCs are considered to be important during the early inflammatory phase of wound healing (Lau et al. 2009), and MSCs release cytokines capable of activating skin cells (Wu et al. 2010). The inflammatory response causes recruitment and activation of many cell types and must be tightly regulated for the subsequent stages of proliferation to be initiated. Moreover, several reports have shown that MSCs enhance wound closure, vasculature, and the thickness of granulation tissue (Wu et al. 2010). Our data demonstrate that EMPB treatment of wounds *in vivo* promoted granulation tissue formation and angiogenesis, as observed by histological examination of healed wound sections. Other skin cell types also contribute to the wound healing process (Broughton et al. 2006), as evidenced by the EMPB-mediated induction of migration in fibroblasts, keratinocytes, and vascular endothelial cells. In the current study, a comparison of the maximum efficacy dose on migration indicated that MSCs had a higher sensitivity toward EMPB than other cell types. In addition, EMPB did not affect collagen production in fibroblasts or the proliferation of vascular endothelial cells. These results suggest that the mobilization of MSCs by EMPB may partially affect wound healing; additional studies are required to confirm that EMPB-induced MSC migration can directly promote regeneration by MSC-derived molecules or differentiation from MSCs into other skin cell types.

In summary, we suggest the following potential cellular mechanisms: (1) administration of EMPB attracts MSCs from the bone marrow or perivascular region into systemic circulation; (2) topical application of EMPB further directs the homing of MSCs from systemic circulation to the wound region; (3) mobilized MSCs proliferate and secrete various cytokines having proregenerative activities; and (4) cytokines activate skin cell types and consequently the activated skin cells, the differentiated cells from MSCs may thus remodel wounded tissues.

Acknowledgements

This work was supported in part by Grants-in-Aid for Scientific Research (C) from the Ministry of Education, Culture, Sports, Science and Technology.

References

Battula, V.L., Evans, K.W., Hollier, B.G., Shi, Y., Marini, F.C., Ayyanan, A., Wang, R.Y., Brisken, C., Guerra, R., Andreeff, M., Mani, S.A., 2010. Epithelial-mesenchymal transition-derived cells exhibit multilineage differentiation potential similar to mesenchymal stem cells. Stem Cells 28, 1435–1445.

Broughton II, G., Janis, J.E., Attinger, C.E., 2006. The basic science of wound healing. Plast. Reconstr. Surg. 117, 12S–34S.

Crisan, M., Yap, S., Casteilla, L., Chen, C.W., Corselli, M., Park, T.S., Andriolo, G., Sun, B., Zheng, B., Zhang, L., Norotte, C., Teng, P.N., Traas, J., Schugar, R., Deasy, B.M., Badylak, S., Buhring, H.J., Giacobino, J.P., Lazzari, L., Huard, J., Peault, B., 2008. A perivascular origin for mesenchymal stem cells in multiple human organs. Cell Stem Cell 3, 301–313.

Fathke, C., Wilson, L., Hutter, J., Kapoor, V., Smith, A., Hocking, A., Isik, F., 2004. Contribution of bone marrow-derived cells to skin: collagen deposition and wound repair. Stem Cells 22, 812–822.

Greenhalgh, D.G., Sprugel, K.H., Murray, M.J., Ross, R., 1990. PDGF and FGF stimulate wound healing in the genetically diabetic mouse. Am. J. Pathol. 136, 1235–1246.

Idowu, T.O., Ogundaini, A.O., Salau, A.O., Obuotor, E.M., Bezabih, M., Abegaz, B.M., 2010. Doubly linked, A-type proanthocyanidin turner and other constituents of *Ixora coccinea* leaves and their antioxidant and antibacterial properties. Phytochemistry 71, 2092–2098.

Kamiyama, K., Watanabe, C., Endang, H., Umar, M., Satake, T., 2001. Studies on the constituents of bark of *Parameria laevigata* moldenke. Chem. Pharm. Bull. 49, 551–557.

Lau, K., Paus, R., Tiede, S., Day, P., Bayat, A., 2009. Exploring the role of stem cells in cutaneous wound healing. Exp. Dermatol. 18, 921–933.

Morikawa, S., Mabuchi, Y., Kubota, Y., Nagai, Y., Niibe, K., Hiratsu, E., Suzuki, S., Miyauchi-Hara, C., Nagoshi, N., Sunabori, T., Shimmura, S., Miyawaki, A., Nakagawa, T., Suda, T., Okano, H., Matsuzaki, Y., 2009. Prospective identification, isolation, and systemic transplantation of multipotent mesenchymal stem cells in murine bone marrow. J. Exp. Med. 206, 2483–2496.

Nishikawa, T., Nakagami, H., Maeda, A., Morishita, R., Miyazaki, N., Ogawa, T., Tabata, Y., Kikuchi, Y., Hayashi, H., Tatsu, Y., Yumoto, N., Tamai, K., Tomono, K., Kaneda, Y., 2009. Development of a novel antimicrobial peptide, AG-30, with angiogenic properties. J. Cell. Mol. Med. 13, 535–546.

Phinney, D.G., Prockop, D.J., 2007. Concise review: mesenchymal stem/multipotent stromal cells: the state of transdifferentiation and modes of tissue repair – current views. Stem Cells 25, 2896–2902.

Sasaki, M., Abe, R., Fujita, Y., Ando, S., Inokuma, D., Shimizu, H., 2008. Mesenchymal stem cells are recruited into wounded skin and contribute to wound repair by transdifferentiation into multiple skin cell type. J. Immunol. 180, 2581–2587.

Sharma, J., Varma, R., 2011. A review on endangered plant of *Mallotus philippensis* (Lam.) M.Arg. Pharmacologyonline 3, 1256–1265.

Tamai, K., Yamazaki, T., Chino, T., Ishii, M., Otsuru, S., Kikuchi, Y., Iinuma, S., Saga, K., Nimura, K., Shimbo, T., Umegaki, N., Katayama, I., Miyazaki, J., Takeda, J., McGrath, J.A., Uitto, J., Kaneda, Y., 2011. PDGFRalpha-positive cells in bone marrow are mobilized by high mobility group box 1 (HMGB1) to regenerate injured epithelia. Proc. Natl. Acad. Sci. U. S. A. 108, 6609–6614.

Umezawa, A., Maruyama, T., Segawa, K., Shadduck, R.K., Waheed, A., Hata, J., 1992. Multipotent marrow stromal cell line is able to induce hematopoiesis in vivo. J. Cell. Physiol. 151, 197–205.

Vojtassak, J., Danisovic, L., Kubes, M., Bakos, D., Jarabek, L., Ulicna, M., Blasko, M., 2006. Autologous biograft and mesenchymal stem cells in treatment of the diabetic foot. Neuro. Endocrinol. Lett. 27, 134–137.

Wagner, J., Kean, T., Young, R., Dennis, J.E., Caplan, A.I., 2009. Optimizing mesenchymal stem cell-based therapeutics. Curr. Opin. Biotechnol. 20, 531–536.

Wang, H., Liu, T.Q., Guan, S., Zhu, Y.X., Cui, Z.F., 2008. Protocatechuic acid from *Alpinia oxyphylla* promotes migration of human adipose tissue-derived stromal cells in vitro. Eur. J. Pharmacol. 599, 24–31.

Wang, H., Liu, T.Q., Zhu, Y.X., Guan, S., Ma, X.H., Cui, Z.F., 2009. Effect of protocatechuic acid from *Alpinia oxyphylla* on proliferation of human adipose tissue-derived stromal cells in vitro. Mol. Cell. Biochem. 330, 47–53.

Wu, Y., Zhao, R.C., Tredget, E.E., 2010. Concise review: bone marrow-derived stem/progenitor cells in cutaneous repair and regeneration. Stem Cells 28, 905–915.